On the importance of cascading moisture recycling in South America

D. C. Zemp[1,2]**, C.-F. Schleussner**[1,3]**, H. M. J. Barbosa**[4]**, R. J. van der Ent**[5]**, J. F. Donges**[1,6]**, J. Heinke**[1]**, G. Sampaio**[7]**, and A. Rammig**[1]

[1]Potsdam Institute for Climate Impact Research (PIK), Telegraphenberg A 31, 14473 Potsdam, Germany
[2]Department of Geography, Humboldt Universität zu Berlin, Berlin, Germany
[3]Climate Analytics, Berlin, Germany
[4]Instituto de Física, Universidade de São Paulo, São Paulo, S.P., Brazil
[5]Department of Water Management, Faculty of Civil Engineering and Geosciences, Delft University of Technology, Delft, the Netherlands
[6]Stockholm Resilience Centre, Stockholm University, Kräftriket 2B, 114 19 Stockholm, Sweden
[7]Center for Earth System Science (CCST), INPE, Cachoeira Paulista, S.P., Brazil

Correspondence to: D. C. Zemp (delphine.zemp@pik-potsdam.de)

Abstract. Continental moisture recycling is a crucial process of the South American climate system. In particular, evapotranspiration from the Amazon basin contributes substantially to precipitation regionally as well as other remote regions such as the La Plata basin. Here we present an indepth analysis of South American moisture recycling mechanisms. In particular, We quantify the importance of "cascading moisture recycling" (CMR), which describes moisture transport between two locations on the continent that involves re-evaporation cycles along the way. Using the Water Accounting Model 2-layers (WAM-2layers) forced by a combination of several climate datasets, we were able to construct a complex network of moisture recycling for South America. Our results show that CMR contributes about 9 – 10 % to the total precipitation over South America and 17 – 18 % over the La Plata basin. CMR increases the fraction of total precipitation over the La Plata basin that comes from the Amazon basin from 18 – 23 to 24 – 29 % during the wet season. We also show that the south-western part of the Amazon basin is not only a direct source of rainfall over the La Plata basin, but also a key intermediary region which distributes moisture originating from the entire Amazon basin towards the La Plata basin during the wet season. Our results suggest that land-use change in this region might have a stronger impact on downwind rainfall than previously thought. Using complex network analysis techniques, we find the eastern flank of the subtropical Andes to be a key region for southward moisture transport via CMR. This study offers a better understanding of the feedbacks between the vegetation and the atmosphere on the water cycle, which is needed in a context of land-use and climate change in South America.

1 Introduction

Continental moisture recycling, the process by which evapotranspiration from the continent returns as precipitation to the continent (Brubaker et al., 1993; Eltahir and Bras, 1994; van der Ent et al., 2010) is particularly important for the South American hydrological cycle. In the Amazon basin, between 25 and 35 % of the moisture is regionally recycled (Eltahir and Bras, 1994; Trenberth, 1999; Bosilovich and Chern, 2006; Burde et al., 2006; Dirmeyer et al., 2009). The moisture from the Amazon basin is also exported out of the basin and transported via the South American Low Level Jet along the Andes. It contributes to precipitation over the La Plata basin particularly during the wet season (Marengo, 2005; Drumond et al., 2008, 2014; Arraut and Satyamurty, 2009; Dirmeyer et al., 2009; van der Ent et al., 2010; Arraut et al., 2012; Martinez et al., 2014).

Land-use change – in particular deforestation in the Amazon basin – alters the evapotranspiration rate and affects the water cycle (see review in Marengo, 2006). A resulting reduction in regional moisture supply may have important consequences for the stability of Amazon rainforests (Oyama

and Nobre, 2003; Cox et al., 2004; Betts et al., 2004; Hirota et al., 2011; Knox et al., 2011; Spracklen et al., 2012).

Downwind rainfall reduction, e.g., in the La Plata basin, may have negative effects on rainfed agriculture (Rockström et al., 2009; Keys et al., 2012). Even if regional impact of changes in precipitation patterns from deforestation has been intensively studied using simulations from atmospheric general circulation models with deforestation scenarios (Lean and Warrilow, 1989; Shukla et al., 1990; Nobre et al., 1991, 2009; Werth and Avissar, 2002; Sampaio et al., 2007; Da Silva et al., 2008; Hasler et al., 2009; Walker et al., 2009; Medvigy et al., 2011; Bagley et al., 2014) the magnitude of rainfall reduction and the location of the most affected regions are still uncertain. In order to improve predictability of rainfall changes with future land-use and climate change, further advancement in our understanding of continental moisture recycling in South America is needed.

To identify the sources and sinks of continental moisture and to quantify regional and continental moisture recycling rates in South America, several methods have been used including isotopes (Salati et al., 1979; Gat and Matsui, 1991; Victoria et al., 1991), atmospheric bulk models (Brubaker et al., 1993; Eltahir and Bras, 1994; Trenberth, 1999; Burde et al., 2006) and quasi-isentropic back-trajectory method (Dirmeyer et al., 2009; Spracklen et al., 2012; Bagley et al., 2014). In addition, numerical atmospheric moisture tracking allows to identify the spatial distribution of evapotranspiration from a specific region. It has been performed online with a general circulation model (GCM) (Bosilovich and Chern, 2006) or a posteriori (offline) with reanalysis data (Sudradjat et al., 2002; van der Ent et al., 2010; Keys et al., 2012) (see a review of the methods in van der Ent et al., 2013; Burde and Zangvil, 2001).

In most of the previous atmospheric moisture tracking studies, moisture from a group of grid cells covering a region of interest (typically the continent) is tracked simultaneously until it returns to the land surface as precipitation or leaves the domain. This approach is useful to investigate how evapotranspiration from a specific location is transported in the atmosphere and precipitates at first in another location. However, precipitating moisture can be re-evapotranspired in the same location (re-evaporation cycle) and can be transported further downwind before it falls again as precipitation over land. In most of the previous studies, only moisture recycling with no intervening re-evaporation cycles ("Direct Moisture Recycling, DMR") is considered. Here, we track moisture evaporating from each grid cell within a larger the domain (i.e., the South American continent) individually. By doing so, we are able to diagnose for each grid cell the amount of evaporating moisture that precipitates in any other cell, i.e., to build a moisture recycling network. Such an approach enables us to study the DMR between important subregions of the South American continent (e.g., the Amazon and the La Plata Basin), but also the moisture transport that

involves at least one re-evaporation cycle ("cascading moisture recycling, CMR").

While only a few previous studies deal with the importance of CMR (Numaguti, 1999; Goessling and Reick, 2013), these studies are based on general circulation models rather than on observation-based data. In the following, we quantify the importance of CMR for the regional climate in South America using numerical atmospheric moisture tracking a posteriori with historical climatological datasets. Our analysis is based on precipitation, evapotranspiration, wind and humidity datasets from a combination of observation-based, reanalysis and merged synthesis products (based on the average of several existing products).

Our network based approach allows us to apply analysis methods developed in complex network theory to improve our understanding of moisture recycling pathways in South America. The potential of complex network based analysis of the climate system has been shown in a range of applications such as the detection of teleconnections (Tsonis et al., 2008; Donges et al., 2009a,b), the propagation of extreme events (Malik et al., 2012; Boers et al., 2013) and the El Niño forecasting (Ludescher et al., 2013). While previous network based studies rely on statistical analysis in the network construction, our approach is based on a flux-based network, which represents a substantial methodological advancement.

In this study we focus on three key questions:

1. what is the importance of CMR in South America and in particular for the moisture transport from the Amazon basin towards the La Plata basin?

2. Which are the important intermediary regions for the transport of moisture from sources and sinks on the continent?

3. Which are the key regions where the pathways of CMR are channeled?

In Sect. 2.1 we describe the tagged water experiment using the WAM-2layers and we explain how we use it to build moisture recycling networks. We explain the assumptions made in the proposed analysis in Sect. 2.2. We develop new measures in Sects. 2.3 and 2.4 and we present the complex network analysis in Sect. 2.5. After comparing the continental and regional recycling ratios with other existing studies in Sect. 3.1, we present and discuss new results on the importance of CMR in Sect. 3.2 and on complex network analysis in Sect. 3.3. Finally, we present an in-depth analysis of the moisture recycling between the Amazon basin and the La Plata basin in Sect. 3.4. As many terms have been introduced in this study, we suggest the reader to refer to the glossary in Appendix A.

2 Methods

2.1 Building moisture recycling networks

2.1.1 Description of the moisture tagging experiment in WAM-2layers

In this study we make use of the Eulerian atmospheric moisture tracking model Water Accounting Model – 2 layers (WAM-2layers) 2.3.01 (van der Ent et al., 2014). It is an update of a previous version that has been used in a variety of publications focusing on moisture tracking and moisture recycling (e.g. van der Ent et al. (2010); van der Ent and Savenije (2011); Keys et al. (2012)). The actual tracking in WAM-2layers is performed a posteriori with two different datasets (see input data in Sect. 2.1.2). Evapotranspiration from each grid cell is "tagged" and subsequently tracked in the atmosphere by applying water balance principles to each grid cell, consisting of a well-mixed upper and lower part. The two-layer approach is simplified compared to full-3-D tracking, but was shown to perform comparably well (van der Ent et al., 2013).

The WAM-2layers runs on a 1.5° longitude/latitude grid. Because the local moisture recycling (re-evaporation cycles) is scale-dependent, the amount of locally recycled moisture within a grid cell depends on the spatial resolution of the model (van der Ent and Savenije, 2011, Fig. 4). However, in our study, the re-evaporation cycles are occurring along the pathway of moisture recycling. Since we are integrating over all pathways contributing to the large-scale moisture transport, the spatial resolution has little influence on our results. The typical length scale of direct links in moisture recycling is larger than 1000 km (c.a. 9°) in the region (van der Ent and Savenije, 2011, Fig. 5), which indicates that our resolution is sufficient to analyze the processes of interest.

We omitted the first year of the considered period from the results because of model spin-up. The output are aggregated first to monthly, then to seasonally average imports and exports between all land grid cells. This temporal resolution is reasonable for our purpose since the time scale of moisture recycling does not exceed 30 days in the studied region (van der Ent and Savenije, 2011, Fig. 5).

These seasonal averages are used to build two seasonal moisture recycling networks, which are assumed to be static for the whole season. This implies that in the proposed analysis, for each season moisture is tracked forward and backward in space but not in time.

2.1.2 Input of WAM-2layers

In order to reduce the uncertainty associated with the input data, we used two different datasets as input for WAM-2layers (that we call "input MOD" and "input LFE", see Table 1). The input MOD covers the period 2000 – 2010 and contains 3 hourly precipitation estimates from the Tropical Rainfall Measuring Mission (TRMM) based on the algorithm 3B-42 (version 7) (Huffman et al., 2007) and 8 days evapotranspiration estimates from Moderate Resolution Imaging Spectroradiometer (MODIS) based on the MOD16 ET algorithm (Mu et al., 2011). Precipitation dataset from TRMM are considered to be reliable over South America and in particular in the Amazon basin where others products perform poorly due to the lack of ground based measurements (Franchito et al., 2009; Rozante et al., 2010). TRMM precipitation data are shown to represent high frequency variability sufficiently well (Kim and Alexander, 2013). However, it is systematically biased during the dry season in the northeastern coast of Brazil, where precipitation is underestimated (Franchito et al., 2009) and at the junction of Argentina, Paraguay and Brazil, where it is overestimated (Rozante and Cavalcanti, 2008). Evapotranspiration from MODIS is estimated using the Penman–Monteith equation (Monteith et al., 1965) forced by satellite and meteorological reanalysis data. Like other "observation-based" evapotranspiration estimations, the quality of the MODIS dataset depends on the quality of the forcing data and the parameterization of the algorithm. The MODIS evapotranspiration dataset has been validated with 10 eddy flux towers located in the Amazonian region under various land cover types (Loarie et al., 2011; Ruhoff, 2011).

The input LFE covers the period 1989 – 1995 and contains monthly evapotranspiration averaged from 39 different products (LandFlux-Eval, Mueller et al. (2013)), as well as monthly precipitation averaged from four different observation-based precipitation datasets: Climate Research Unit (CRU) (New et al., 2000), the Global Precipitation Climatology Centre (GPCC) (Huffman et al., 1995; Adler et al., 2003), GPCP (Adler et al., 2003) and the unified climate prediction center (CPC) from the National Oceanic and Atmospheric Administration (NOAA) (Chen et al., 2008). The four precipitation datasets are interpolations from rain gauge data (in combination with satellite observation in the case of GPCC) and have been used as forcing dataset for the "observation-based" evapotranspiration product in LandFlux-Eval (Mueller et al., 2013). Here, we include the evapotranspiration products in LandFluxEval that are not only derived from observations, but also calculated via landsurface models and output from reanalysis.

Both datasets are complemented by 6 hourly specific humidity and wind speed in three dimensions from the ERA-Interim reanalysis product (Dee et al., 2011) for the corresponding periods. Because these two variables are used to get the horizontal moisture fluxes, the choice of the reanalysis product matters for the eventual results of the WAM-2layers (Keys et al., 2014). Humidity estimation has been improved in the ERA-Interim product in comparison with others reanalysis products (Dee and Uppala, 2008).

The temporal resolution of the input data needed in WAM-2layers is 3 hours. Therefore, we downscaled the input MOD and 2 based on the temporal dynamic found in the ERA-

Interim evapotranspiration and precipitation products. In addition, all data is downscaled to 0.5 h as requested by the numerical scheme of WAM-2layers. All data is upscaled to a regular grid of 1.5° longitude/latitude and covers the South American continent to 50° S, which is the southernmost latitude covered by TRMM product.

The long term seasonal average of evapotranspiration and precipitation as well as moisture flux divergence (evapotranspiration – precipitation) are shown in Figs. 4 and 5. The high rainfall in the South Atlantic Convergence Zone (including the Amazon basin, central and south-eastern Brazil) during the wet season (December to March) compared to the dry season (June to September) characterizes the South American Monsoon System (SAMS) (Liebman et al., 1999; Grimm et al., 2004; Arraut and Satyamurty, 2009).

The evapotranspiration and precipitation in the input MOD have an overall positive bias compared to the input LFE. While the spatial patterns of evapotranspiration show good agreement on a continental scale, there are also several distinct differences. In particular the wet season evapotranspiration in the sub-tropical South America is much weaker in the input MOD then LFE. Interpreting and explaining the differences between the datasets is beyond the scope of this study. For an evaluation of the different types of products (model calculation, "observation-based" and reanalysis), we refer to Mueller et al. (2011).

In both inputs the evapotranspiration exceeds the total precipitation in the southern part of the Amazon basin during the dry season, indicating that this region is a net source of moisture for the atmosphere (Fig. 4c and 5c). This is in agreement with previous studies demonstrating a maintaining of the greenness of the Amazon forests (Morton et al., 2014) and the absence of water stress during the dry season due to the deep root system, which enables the pumping of the water from the deeper water table (Nepstad et al., 1994; Miguez-Macho and Fan, 2012).

We find that, averaged over the full time period, evapotranspiration exceeds precipitation in northeastern Brazil and in the Atacama Desert in both datasets, as well as along the Andes in the input MOD. Possible explanations for the imbalance in these arid to semi-arid regions are irrigation or biases in the input data as mentioned above. As this might lead to a bias in moisture recycling ratios due to an overestimation of the contribution of evapotranspiration to local precipitation, we will exclude these grid cells from our analysis.

2.1.3   Construction of a complex network based on WAM-2layers

The output of WAM-2layers is a matrix $\mathbf{M} = \{m_{ij}\}$ for all $i, j \in N$ with N the number of grid cells in the continent ($N = 681$). The non-diagonal element m_{ij} is the amount of evapotranspiration in grid cell i that precipitates in grid cell j and the diagonal element m_{ii} is the amount of evapotranspiration that precipitates in the same grid cell (locally recycled

moisture). The output of WAM-2layers can be interpreted as the adjacency matrix of a directed and weighted complex network with self-interactions, where nodes of the network represent grid cells and links between nodes represent the direction and amount of moisture transported between them (Fig. 1).

2.2   Basic assumptions

In order to track moisture forward or backward from a given region Ω that can be of any shape and scale (grid cell, basin, continent), we assume that the moisture composition within the surface reservoir and the atmosphere for each grid cell remains the same. This implies that, in each grid cell, the tagged fraction of precipitation is linearly proportional to the tagged fraction of evapotranspiration and the tagged fraction of transported moisture:

$$\frac{P_\Omega}{P} = \frac{E_\Omega}{E} = \frac{m_\Omega}{m}, \tag{1}$$

where E is the total evapotranspiration, P is the total precipitation, m is the transported moisture towards or from another grid cell, P_Ω is the tagged fraction of precipitation, E_Ω is the tagged fraction of evapotranspiration and m_Ω is the tagged fraction of transported moisture towards or from another grid cell. We call "tagged fraction" the share of the moisture originating from Ω in the case of a backward tracking and the share of moisture precipitating over Ω in the case of a forward tracking.

This assumption is valid under two conditions: (1), evapotranspiration follows directly after the precipitation event or (2), the fraction of tagged moisture in the surface reservoir and the atmosphere can be assumed to be temporally constant (i.e., in steady state) (Goessling and Reick, 2013). The first condition is usually fulfilled during interception and fast transpiration, which are important components of the total evapotranspiration, particularly in warm climates and for shallow rooted plants (Savenije, 2004). However, in seasonal forests with deep rooted trees, the moisture that is evaporated during the dry season can be hold back for several months (Savenije, 2004). By analyzing a seasonally static moisture recycling network, we account for this limitation. The second condition is fulfilled if the soil water at the beginning has the same composition (in term of tagged fraction) as the atmospheric moisture at the end of the season.

2.3   Moisture recycling ratio

Common measures to quantify the strength of the direct link between precipitation in a specific location and evapotranspiration from another location are the moisture recycling ratios (called hereafter DMR ratio) (Eltahir and Bras, 1994; Trenberth, 1999; Bosilovich and Chern, 2006; Dirmeyer et al., 2009; van der Ent et al., 2010; Keys et al., 2012; Bagley et al., 2014). The DMR ratios are only used to investigate

DMR. Here, we further develop these measures in order to take CMR into account.

2.3.1 DMR (direct moisture recycling) ratios

Two kinds of DMR ratios have been developed in a previous study van der Ent et al. (2010): the direct precipitation recycling ratio and the direct evapotranspiration recycling ratio. The direct precipitation recycling ratio ρ_Ω has been defined as the fraction of precipitation that is originating from evapotranspiration from a defined region Ω with no intervening re-evaporation cycle (see also Appendix C1.1). We note that ρ_Ω averaged over all grid cells in Ω gives the regional recycling ratio, i.e, the fraction of precipitation that is regionally recycled (Eltahir and Bras, 1994; Burde et al., 2006; van der Ent and Savenije, 2011). High values of ρ_Ω indicate the "direct sink regions" of evapotranspiration from Ω, i.e., the regions that are dependent on evapotranspiration coming directly (i.e., through DMR) from Ω for local precipitation. A direct sink region receives moisture from Ω at first and might distribute it further downwind (Fig. 2).

Similarly, the direct evapotranspiration recycling ratio ε_Ω has been defined as the fraction of evapotranspiration that falls as precipitation over a defined region Ω with no intervening re-evaporation cycle (see also Appendix C1.1). High values indicate the "direct source regions" of precipitation over Ω, i.e., the regions that contribute directly (i.e., through DMR) to rainfall over Ω. A direct source region distributes moisture towards Ω, which might be originating from further up-wind regions (Fig. 2).

If Ω is the entire South American continent, ε_Ω becomes the continental evapotranspiration recycling ratio (ε_c) and ρ_Ω the continental precipitation recycling ratios (ρ_c) as defined in van der Ent et al. (2010). Considered together, ε_c and ρ_c indicate respectively sources and sinks of continental moisture. In this study we neglect possible contributions of moisture in South America from and to other continents, since these contributions to the overall moisture budget are small (van der Ent et al., 2010, Table 2).

2.3.2 CMR (cascading moisture recycling) ratios

We define the cascading precipitation recycling ratio $\rho_\Omega^{\mathrm{casc}}$ as the fraction of precipitation that is originating from evapotranspiration from Ω and that has run through at least one re-evaporation cycle on the way (see also Appendix C1.2). High values indicate the "cascading sink regions" of evapotranspiration from Ω, i.e., the regions that are dependent on evapotranspiration coming indirectly (i.e., through CMR) from Ω for local precipitation. A cascading sink region is the last destination of evapotranspiration from Ω before it is advected over the ocean (Fig. 2).

We also define the cascading evaporation recycling ratio $\varepsilon_\Omega^{\mathrm{casc}}$ as the fraction of evapotranspiration that falls as precipitation over Ω after at least one re-evaporation cycle on the way (see also Appendix C1.2). High values indicate the "cascading source regions" of precipitation over Ω, i.e., the regions that contribute indirectly (i.e., through CMR) to rainfall over Ω. A cascading source region is the origin of moisture that is distributed from somewhere else towards Ω (Fig. 2).

The moisture inflow (resp. outflow) that crosses the border of Ω may be counted several times as it is involved in several pathways of CMR. To avoid this, we only track moisture that crosses the border of Ω. This implies that we consider re-evaporation cycles outside Ω only (Fig. 2, see also Appendix C1.2).

2.3.3 Application to the Amazon basin and the La Plata basin

To study the moisture recycling between the Amazon basin and the La Plata basin (defined by the red boundaries in Fig. 8), we use ρ_Ω and $\rho_\Omega^{\mathrm{casc}}$ with Ω being all grid cells covering the Amazon basin (ρ_{Am} and $\rho_{\mathrm{Am}}^{\mathrm{casc}}$ respectively) and ε_Ω and $\varepsilon_\Omega^{\mathrm{casc}}$ with Ω being all grid cells covering the La Plata basin ($\varepsilon_{\mathrm{Pl}}$ and $\varepsilon_{\mathrm{Pl}}^{\mathrm{casc}}$ respectively). High values of ρ_{Am} and $\rho_{\mathrm{Am}}^{\mathrm{casc}}$ indicate together the sink regions of evapotranspiration from the Amazon basin and high values of $\varepsilon_{\mathrm{Pl}}$ and $\varepsilon_{\mathrm{Pl}}^{\mathrm{casc}}$ highlight source regions of precipitation over the La Plata basin (Fig. 2).

Considered together, the DMR ratios and the CMR ratios ratios provide a full picture of the source - sink relationship between the Amazon basin and the La Plata basin that is needed to estimate the effects of land-use change for downwind precipitation patterns. $\rho_{\mathrm{Am}}^{\mathrm{casc}}$ and ρ_{Am} quantify the local dependency on incoming moisture from the Amazon basin (with and without re-evaporation cycles) and therefore the local vulnerability to deforestation in the Amazonian rainforests. Considering ρ_{Am} only would lead to underestimation of this dependency. On the other hand, $\varepsilon_{\mathrm{Pl}}$ and $\varepsilon_{\mathrm{Pl}}^{\mathrm{casc}}$ provide information on the upwind regions that contribute to rainfall over the La Plata basin and, consequently, that should be preserved from intensive land-use change in order to sustain water availability in the La Plata basin.

2.4 Quantifying CMR (cascading moisture recycling)

To quantify the importance of CMR for the total moisture inflow (precipitation, P) and outflow (evapotranspiration, E), we cut-off all re-evaporation of moisture originating from the continent and we estimate the resulting reduction in total moisture inflow (ΔP_c) and outflow (ΔE_c) (see Appendix C2). $\Delta P_c/P$ is the fraction of precipitation that comes from re-evaporation of moisture originating from the continent, i.e., that has been evaporated in at least two locations on the continent. $\Delta P_c/P$ quantifies the importance of CMR for local rainfall. $\Delta E_c/E$ is the fraction of total evapotranspiration that is a re-evaporation of moisture originating from the continent and that further precipitates over the continent, i.e.,

that lies within CMR pathways. $\Delta E_{\mathrm{c}}/E$ quantifies the local contribution to CMR. High values of $\Delta E_{\mathrm{c}}/E$ indicate intermediary regions. Regions that have a larger $\Delta E_{\mathrm{c}}/E$ than the 80 percentile (calculated for all seasonal values over the continent) are called "intermediary" regions in the following.

In addition, we are interested in the importance of re-evaporation cycles that are occurring in the intermediary regions for the total moisture in- and outflow. We use the same approach as above. We cut-off all re-evaporation in the intermediary region of moisture originating from the continent and we estimate the resulting reduction in total moisture inflow (ΔP_{m}) (see Appendix C2). $\Delta P_{\mathrm{m}}/P$ is the fraction of total moisture inflow that comes from CMR in the intermediary region (i.e., that has run through at least one re-evaporation cycle in the intermediary region). It quantifies the dependency on CMR in the intermediary region for local rainfall.

2.5 Complex network analysis

We investigate important moisture recycling pathways using two measures from complex network analysis: clustering coefficient associated with Middleman motifs and betweenness centrality.

2.5.1 Clustering coefficient associated with Middleman motifs ($\tilde{C}$)

In complex network theory, motifs are defined as significant and recurring patterns of interconnections that occur in the network (Milo et al., 2002). Here, we are interested in a particular pattern of directed triangles: the Middleman motif (Fagiolo, 2007). In our study, a grid cell forms a Middleman motif if it represents an intermediary on an alternative pathway to the direct transport of moisture between two other grid cells (Fig. 3).

The clustering coefficient is a measure from complex network analysis that measures the tendency to form a particular motif (Fagiolo, 2007). Here, it reveals intermediary locations in CMR pathways, as the alternative to the DMR between sources and sinks. To account for moisture fluxes along the network links, we compute the weighted version of the clustering coefficient associated with Middleman motifs ($\tilde{C}$) (Fagiolo, 2007; Zemp et al., 2014) for each grid cell as described in the Appendix C3.1.

A grid cell has a high $\tilde{C}$ if it forms a lot of Middleman motifs and if these motifs contribute largely to relative moisture transport. $\tilde{C}$ is equal to zero if the grid cell forms no Middleman motif at all.

It is worth to note that the Middleman motif considers three interconnected grid cells, which corresponds to CMR pathways involving only one re-evaporation cycle. These pathways contribute usually most to moisture transport between two locations. In fact, the amount of moisture transported in a pathway typically decreases with the number of re-evaporation cycles involved in the pathway. This is in agreement with a previous study counting the number of re-evaporation cycles using a different methodology (Goessling and Reick, 2013). Other motifs formed by three or more grid cells linked by moisture recycling exist (Zemp et al., 2014), but are not analyzed here.

2.5.2 Betweenness centrality (B)

B aims to highlight nodes in the network with central position "to the degree that they stand between others and can therefore facilitate, impede or bias the transmission of messages" in the network (Freeman, 1977, p. 36). Here, we use it to reveal intermediary grid cells where CMR pathways are channeled.

To compute it, we first identify for each pair of grid cells the moisture recycling pathways with the greatest throughput, called "optimal pathways' (see Appendix C3.2). These pathways can include any number of re-evaporation cycles. As the optimal pathway is usually the direct one (without any re-evaporation cycle), we first had to modify the network such that the optimal pathways involve re-evaporation cycles. To do so, we removed from the network all long-range moisture transport, i.e., occurring over distances larger than 15 geographical degrees. The choice of this threshold does not influence the results qualitatively on a yearly basis (Fig. B4). During the dry season, removing long-range affects moisture inflow over the La Plata basin, therefore the results of the B will be interpreted with caution during this season.

Once optimal pathways are identified, we find intermediary grid cells that they have in common (see Appendix C3.3). A grid cell has a high B if many optimal pathways pass through it, i.e., moisture runs often through re-evaporation cycle in the grid cell, and has a B equal to 0 if none of these pathways pass through it, i.e., moisture never runs through re-evaporation cycle in the grid cell.

2.6 Similarities and differences between the presented measures

We expect similar spatial patterns in the results of $\Delta E_{\mathrm{c}}/E$ (fraction of evapotranspiration that lies within CMR pathways, see Sect. 2.4), the B (betweenness centrality, see Sect. 2.5.2) and the $\tilde{C}$ (clustering coefficient, Sect. 2.5.1). In fact, all three measures reveal important intermediary grid cells in CMR pathways. However, the three measures are based on different concepts and methods.

1. While $\Delta E_{\mathrm{c}}/E$ is calculated by inhibiting re-evaporation of moisture from continental origin, B is based on the notion of optimal pathways and $\tilde{C}$ relies on particular motifs formed by three connected grid cells.

2. An implication of (1) is that $\Delta E_{\mathrm{c}}/E$ quantifies the local contribution to CMR, $\tilde{C}$ refers to CMR pathways as alternative to the direct transport of moisture between

two locations and B shows locations where CMR pathways are channeled.

3. In the $\tilde{C}$, only CMR pathways with one re-evaporation cycle are considered. Using $\Delta E_c/E$ and B, all number of cycles are possible in the pathways.

4. Moisture recycling pathways involving long-range transport are not considered in the calculation of the B.

For these reasons, $\Delta E_c/E$, B and $\tilde{C}$ are complementary measures. There are also some similarities between the calculation of the cascading precipitation recycling ratio and $\Delta P_c/P$, which are described in the appendix C1.3.

3 Results and discussion

3.1 Comparison of continental and regional moisture recycling ratios with other existing studies

The main continental source of precipitation in South America is the Amazon basin, with large heterogeneity in time and space (Figs. 4e, 4j, 5e and 5j and Table 3). 70 to 80 % of the evapotranspiration in the southern part of the Amazon basin falls as precipitation over the continent during the wet season but only 30 to 40 % during the dry season. As the evapotranspiration in the Amazon basin is high and varies little in space and time (Figs. 4b, 4g, 5b and 5g), this observation indicates that during the dry season, a high amount of moisture from the southern part of the Amazon basin is advected out of the continent. Using a Lagrangian particle dispersion model, Drumond et al. (2014) also found a maximum contribution of moisture from the Amazon basin to the ocean during this period.

The main sink regions of moisture originating from the continent are the western part of the Amazon basin during the dry season, the south-western part of the basin during the wet season and the La Plata basin especially during the wet season (Figs. 4d, 4i, 5d and 5di and Table 3). In fact, in the La Plata basin, 42 to 45 % of the precipitation during the wet season and 35 % during the dry season evaporated from the continent. This difference between seasons is explained by a weaker transport of oceanic moisture associated with the subtropical Atlantic high and by an intensification of the South American Low-Level Jet (SALLJ) that transports moisture in the meridional direction during this season (Marengo et al., 2004). The importance of continental moisture recycling in the La Plata basin during the wet season has been emphasized in previous studies (Drumond et al., 2008; Martinez et al., 2014). Despite this importance, we find that the ocean remains the main source of moisture over the La Plata basin in agreement with previous studies (Drumond et al., 2008; Arraut and Satyamurty, 2009; Drumond et al., 2014). However, some other studies estimated a higher contribution of moisture from the continent to precip-

itation over the La Plata basin van der Ent et al. (2010); Keys et al. (2012); Martinez et al. (2014).

There are uncertainties in the moisture recycling ratios depending on the quality of the datasets used, the assumptions made in the methods and the boundaries used to define the domain (for example in Brubaker et al., 1993, the Amazon region is represented by a rectangle). Considering these uncertainties, the regional precipitation recycling ratio in the Amazon basin compares well with previous studies using other datasets and methodologies (See Table 2). The spatial patterns of continental moisture recycling ratios (Figs. 4d, 4i, 4e, 4j, 5d, 5i, 5e and 5j) are slightly different from those found by (van der Ent et al., 2010, Figs. 3 and 4) due to the differences in the versions of the model (here we use WAM-2layers) and the datasets used. The continental precipitation recycling ratio in the Amazon basin reaching 27 to 30 % during the Southern Hemisphere summer is slightly below estimates by the estimate of 36.4 % found by Bosilovich and Chern (2006). The maps of DMR ratios (Fig. 8c, and g, a and e) are in good agreement with regional recycling ratio reported in previous studies (Eltahir and Bras, 1994, Figs. 4 and 6 and Burde et al., 2006, Figs. 2 and 8 and Dirmeyer et al., 2009 see http://www.iges.org/wcr/, Moisture Sources by Basin).

We note that our analysis period from 2001–2010 (for the input MOD) includes two major droughts in the Amazon basin (Marengo et al., 2008; Lewis et al., 2011). Because the land–atmosphere coupling on the hydrological cycles increases during drought years (Bagley et al., 2014), this might influence the output of the atmospheric moisture tracking model used in this study. Analyzing these periods separately is ongoing research.

3.2 Importance of CMR (cascading moisture recycling)

Continental moisture recycling is of crucial importance for South American precipitation patterns (Figs. 4 and 5). We now quantify this importance (Figs. 6 and B1).

The share of cascading moisture on total moisture inflow is on average 9 – 10 % in the South American continent (Table 3). Regions that are dependent on CMR for local rainfall (Figs. 6a, 6c, B1a and B1c) are also dominant sinks of moisture from the continent (Figs. 4d, 4i, 5d and 5i).

We note that CMR contributes more to the precipitation over the Amazon basin during the dry season (8 – 11 % on average, up to 25 % in the western part) compared to the wet season (6 – 8 % on average). This is explained by the fact that during the dry season, moisture is mainly transported from the eastern to the western part of the Amazon basin (Figs. 4 and (Figs. 5). Our results show that during the dry season, this moisture transport involves re-evaporation cycles in the central part of the basin (blue boundaries in Figs. 6b and B1d). In fact, 15 – 23 % of the total evapotranspiration from the Amazon basin is involved in CMR during the dry season.

During the wet season, CMR plays also an important role as $17 - 18\%$ of the total precipitation over the La Plata basin comes from CMR. The intermediary region where re-evaporation cycles are taking place is mainly the south-western part of the Amazon basin (blue boundaries in Figs. 6d and B1d). In this intermediary region, up to 35% of the total evapotranspiration is involved in CMR during the wet season. We note that the shape of the intermediary regions varies slightly among the two datasets during the wet season, probably explained by the differences in evapotranspiration patterns (Figs. 4g and 5g).

In order to quantify the importance of the intermediary region for rainfall over the La Plata basin, we quantify the share of the moisture inflow in the La Plata basin that has run through re-evaporation cycles in the intermediary regions. This share is $8 - 10\%$ during the wet season and $3 - 4\%$ during the dry season. These estimations represent about half of the share of total moisture inflow over the La Plata basin that comes from CMR during the wet season (Table 3). These results mean that the intermediary regions are important for cascading moisture transported towards the La Plata basin during the wet season. In Sect. 3.4, we reveal the direct and cascading sources of precipitation over the La Plata basin and we understand the seasonal variability.

The share of cascading moisture on the total moisture inflow reaches up to $35 - 50\%$ in the eastern side of the central Andes, one of the most vulnerable biodiversity hotspots on Earth (Myers et al., 2000). However, this latter observation should be considered with caution due to the imbalance of the water cycle in this area, which might lead to an over-estimation of the regional recycling process and thus an over-estimation of the importance of cascading moisture recycling.

3.3 Complex network analysis

We have shown the importance of CMR for South American moisture transport (Fig. 6). Using the clustering coefficient associated with the Middleman motif ($\tilde{C}$), we are able to identify intermediary locations involved in cascading pathways as alternative to the direct transport of moisture (Figs. 7a, 7c, B2a and B2c). These regions coincide with the intermediary regions identified with a different method (blue boundaries in Figs. 6 and B1). These results mean the CMR pathways involving the intermediary regions are not the only pathways of moisture recycled from sources to sinks on the continent, but are complementing the direct transport of moisture over long distances.

The betweenness centrality (B) reveals intermediary regions where CMR pathways are channeled. We note that regions with high B coincide with regions with high $\tilde{C}$ during the wet season, but not as much during the dry season (Figs. 7 and B2). This might be a results of the cutting of long-range links from the network in the calculating of the B, which affects moisture transport towards the subtropical South America during the dry season.

High values of B are found along a narrow band east of the subtropical Andes (Figs. 7d and B2d), indicating that CMR pathways are channeled in this region. This observation may be explained by the combined effect of the acceleration of the South American Low Level Jet (Vera et al., 2006) and the high precipitation and evapotranspiration during the wet season (Figs. 4 and 5) allowing for an intensive local exchange of moisture between the vegetation and the atmosphere.

3.4 Moisture recycling from the Amazon basin to the La Plata basin

We have shown the importance of the Amazon basin as the dominant source of continental moisture and the La Plata basin as a central sink region (see Figs. 4 and 5). In the following, we further investigate the importance of DMR and CMR for the transport of moisture between the two basins (Figs. 8 and B3).

In the La Plata basin, $18 - 23\%$ of the precipitation during the wet season and $21 - 25\%$ during the dry season originated from the Amazon basin with no intervening re-evaporation cycles (Table 3). This is in good agreement with the yearly average estimates of 23% found in Dirmeyer et al. (2009, see http://www.iges.org/wcr/) and 23.9% found in Martinez et al. (2014). Considering CMR increases the fraction of precipitation that comes from the Amazon basin by 6% during the wet season (Figs. 8h and B3h and Table 3). As mentioned above, this might be explained by the high evapotranspiration and precipitation allowing for an exchange of moisture on the way and by the intensification of the SALLJ during this time of the year (Marengo et al., 2004). This result suggests that the impact of deforestation in the Amazonian forest on rainfall over the La Plata basin might be larger than expected if only direct transport of moisture between the two basins are considered.

The southern part of the Amazon basin is a direct source of precipitation over the La Plata basin (Figs. 8a, 8e, B3a and B3e). This finding is in agreement with Martinez et al. (2014) and Keys et al. (2014). However, if CMR is considered, the entire Amazon basin becomes an evaporative source of moisture for the La Plata basin during the wet season (Figs. 8f and Figs. B3f). On average, $16 - 23\%$ of the total evapotranspiration from the Amazon basin during the wet season ends as rainfall over the La Plata basin after at least one re-evaporation cycle (Table 3). This result means that during the wet season, the southern part of the Amazon basin is not only a direct source of moisture for the La Plata basin but also an intermediary region that distributes moisture originating from the entire basin. This finding is in agreement with other measures showing intermediary regions (Sects. 3.2 and 3.3).

3.5 Possible impact of land-cover change in the intermediary regions

The southern part of the Amazon basin is a key region for moisture transport towards the La Plata basin. It is a source of moisture for precipitation over the La Plata basin all year round. In addition, it is an intermediary region in the indirect transport of moisture (through CMR) originating from the entire Amazon basin during the wet season (Sect. 3.4).

Land cover change in the southern part of the Amazon basin might weaken continental moisture recycling and might lead to an important decrease in the total precipitation locally and downwind. Among the affected regions, important impacts would be observed in particular in the south-western part of the Amazon basin that has already a high probability to experience a critical transition from forest to savanna (Hirota et al., 2011) and in the La Plata basin that is dependent on incoming rainfall for the agriculture (Rockström et al., 2009; Keys et al., 2012). In the eastern side of the central Andes, the impact of an upwind weakening of CMR might be reduced since precipitation in this region is insured by orographic lifting (Figueroa and Nobre, 1990).

4 Conclusions

In this work, we investigated the exchange of moisture between the vegetation and the atmosphere on the way between sources and sinks of continental moisture in South America. We have introduced the concept of "cascading moisture recycling" (CMR) to refer to moisture recycling between two locations on the continent that involve one or more re-evaporation cycles along the way. We have proposed measures to quantify the importance of CMR, to track moisture from a given region further backward or forward in space and to identify intermediary regions where re-evaporation cycles are taking place. We have used for the first time a complex network approach to study moisture recycling pathways.

We have tracked moisture evaporating from each grid cell covering the South American continent until it precipitates or leaves the continent using the atmospheric moisture tracking model Water Accounting Model-2layers (WAM-2 layers). In order to reduce the uncertainty associated with the input data, we use two different sets of precipitation and evapotranspiration data from (1) observation-based and (2) merged synthesis products, together with reanalysis wind speeds and humidity data. We have shown that even if the amount of water transported through CMR pathways is typically smaller than the one transported directly in the atmosphere, the contribution by the ensemble of cascading pathways can't be neglected. In fact, 9 – 10 % of the total precipitation over South America and 17 – 18 % of the precipitation over the La Plata basin comes from CMR. The La Plata basin is highly dependent on moisture from the Amazon basin during both seasons, as 18 – 23 % of the total precipitation over the La Plata basin during the wet season and 21 – 25 % during the dry season comes directly from the Amazon basin. To these direct dependencies, 6 % of the precipitation during the wet season can be added if CMR are considered.

During the dry season, CMR plays an important role for the moisture transport from the eastern to the western part of the Amazon basin. Indeed, 16 – 23% of the total evapotranspiration in the Amazon basin is involved in CMR during the dry season.

The south-western part of the Amazon basin is an important direct source of incoming moisture over the La Plata basin all year round. However, during the wet season, it is not only a direct source but also an intermediary region that distributes moisture from the entire Amazon basin into the La Plata basin. Land use change in these regions may weaken moisture recycling processes and may have stronger consequences for rainfed agriculture and natural ecosystems regionally and downwind as previously thought.

In addition, we showed that the eastern flank of the subtropical Andes – located in the pathway of the South American Low Level Jet – plays an important role in the continental moisture recycling as it channels many cascading pathways. This study offers new methods to improve our understanding of vegetation and atmosphere feedback on the water cycle needed in a context of land use and climate change.

Appendix A

Glossary

- **Moisture recycling**: the process by which evapotranspiration in a specific location on the continent contributes to precipitation in another location on the continent.

- **Re-evaporation cycle**: evapotranspiration of precipitating moisture in the same location

- **Cascading moisture recycling (CMR)**: moisture recycling that involves at least one re-evaporation cycle on the way.

- **Direct moisture recycling (DMR)**: moisture recycling with no intervening re-evaporation cycle on the way.

- **Intermediary**: location where moisture runs through re-evaporation cycle on its way between two locations on the continent (only in the case of CMR).

- **Pathway of moisture recycling**: set of locations on land involved in moisture recycling. A DMR pathway includes only the starting (evapotranspiration) and the destination (precipitation) locations, while a CMR pathway includes the starting, the destination and the intermediary locations.

- **Optimal pathway**: the pathway of moisture recycling that contributes most to moisture transport between two locations. It can be a direct or a cascading pathway.

- **Direct source**: land surface that contributes directly (i.e., through DMR) to rainfall over a given region.

- **Cascading source**: land surface that contributes indirectly (i.e., through CMR) to rainfall over a given region.

- **Source**: land surface that contributes directly or indirectly to rainfall over given region.

- **Direct sink**: land surface that is dependent on evapotranspiration coming directly (i.e., through DMR) from a given region for local precipitation.

- **Cascading sink**: land surface that is dependent on evapotranspiration coming indirectly (i.e., through CMR) from a given region for local precipitation.

- **Sink**: land surface that is dependent on evapotranspiration coming directly or indirectly from a given region for local precipitation.

Appendix B

Supplementary figures

Results for the input LFE are presented in Figs. B1, B2 and B3. Fig. B4 shows the B (betweeness centrality) for different thresholds in the geographical distance of the links excluded from the network.
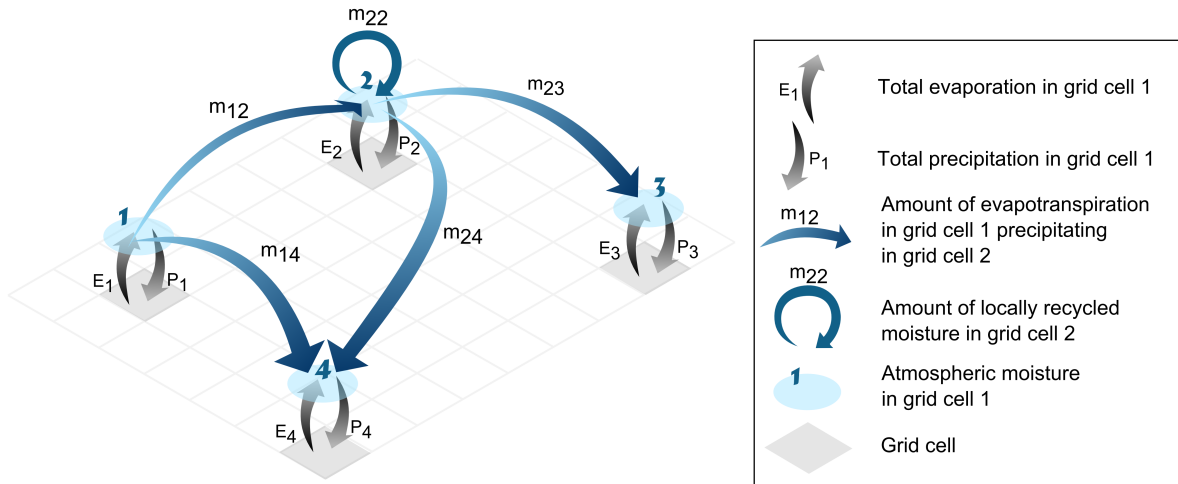
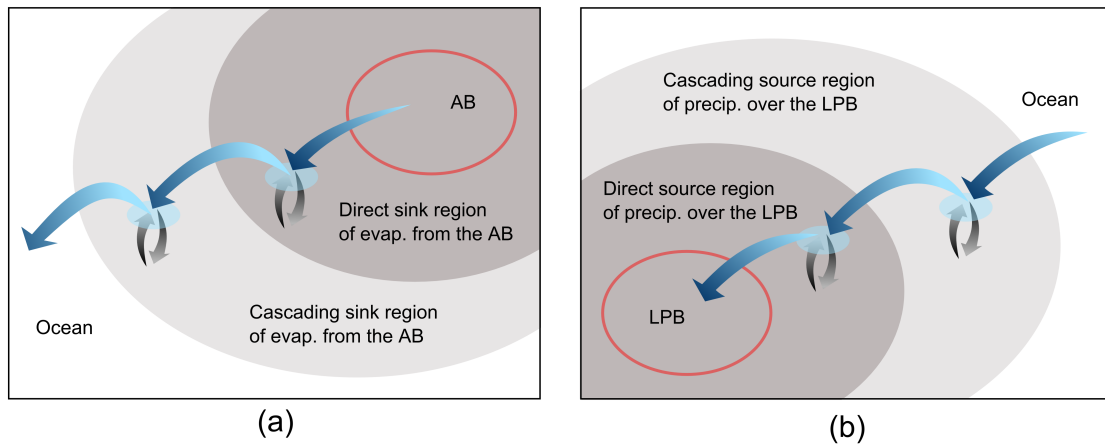Fig. 1: Schematic representation of the moisture recycling network.

Fig. 2: Schematic representation of the sink and sources regions as quantified by the moisture recycling ratios. In addition to the direct source and sink regions identified using DMR ratios (dark gray), the cascading source and sink regions identified using CMR (light gray) are highlighted. Direct and cascading sink regions of evapotranspiration (evap.) from the Amazon basin (AB) (a) and direct and cascading source regions of precipitation (precip.) over the La Plata basin (LPB) (b).

Table 1: Input datasets used for building moisture recycling networks. The first year of the period is omitted from the results because of model spin-up.

Input name	Evapotranspiration product	Precipitation product	Period
Input MOD	MODIS	TRMM	2000 – 2010
Input LFE	LandFlux-Eval	Average of CRU, GPCC, GPCP and CPC	1989 – 1995

Table 2: Overview of regional precipitation recycling ratio in the Amazon basin as found in many studies. Abbreviations: the European Centre for Medium-Range Weather Forecasts (ECMW); Geophysical Fluid Dynamics Laboratory Precipitation (GFDL); Climate Prediction Center Merged Analysis of Precipitation (CMAP); Initital conditions (IC); October-November-December (OND); Data Assimilation Office (DAO); Integral Moisture Balance (IMB) model; NCEP – Department of Energy (DOE); World Monthly Surface Station Climatology distributed by the National Center for Atmospheric Research (NCAR).

Study	Method	Dataset	Period	Precipitation recycling ratio
Brubaker et al. (1993)	Atmospheric Bulk model	GFDL and NCAR	1963–1973	24
Eltahir and Bras (1994)	Atmospheric Bulk model	ECMWF reanalysis	1985–1990	25
		GFDL	1963–1973	35
Trenberth (1999)	Atmospheric Bulk model	CMAP and NCEP-NCAR re-analysis	1979–95	34
Bosilovich and Chern (2006)	AGCM with water vapor tracers	IC from the model	1948–1997	27.2 during OND
Burde et al. (2006)	Atmospheric Bulk model (general)	DAO	1981–1993	31
	Atmospheric Bulk model (Budyko model)			26
	Atmospheric Bulk model (IMB)			41
Dirmeyer et al. (2009)	Quasi-isentropic back-trajectory method	DOE reanalysis	1979–2003	10.8 for area 10^6 km^2
van der Ent et al. (2010)	Atmospheric moisture tracking model	ERA-Interim reanalysis	1999–2008	28
Zemp et al. (this study)	Atmospheric moisture tracking model	TRMM and MODIS	2001–2010	28
Zemp et al. (this study)	Atmospheric moisture tracking model	LandFluxEval and average of CRU,GPCC,GPCP and CPC	1990–1995	24

Appendix C

Supplementary description of the method

In all the measures the irregular sizes of the portion of the Earth's surface covered by the grid cells are taken into account as described in Zemp et al. (2014).

C1 Moisture recycling ratios

C1.1 DMR (direct moisture recycling) ratios

The ρ_Ω in grid cell j is calculated as:

$$\rho_{\Omega,j} = \frac{\sum_{i \in \Omega} m_{ij}}{P_j}, \tag{C1}$$

where m_{ij} is the amount of evapotranspiration in i that precipitates in j with no intervening re-evaporation cycle and P_j is the precipitation in j. The ε_Ω in grid cell i is calculated as:

$$\varepsilon_{\Omega,i} = \frac{\sum_{j \in \Omega} m_{ij}}{E_i}, \tag{C2}$$

where E_i is the evapotranspiration in i.

C1.2 CMR (cascading moisture recycling) ratios

To calculate the CMR ratios as defined in Sect. 2.3.2, we calculate the individual contributions of CMR pathways consisting of k re-evaporation cycles ($k \in \{1, \ldots, n\}$), which add up to the total CMR contribution. We chose a maximum number of cycles $n = 100$, while the contribution of pathways with number of cycles larger than 3 are close to zero.

Table 3: Importance of direct moisture recycling (DMR) and cascading moisture recycling (CMR) for the total precipitation (precip.) and evapotranspiration (evap.) averaged for the La Plata basin (LPB), the Amazon basin (AB) and for the South American continent during the wet season (DJFM), the dry season (JJAS) and all year round calculated for the input MOD / LFE (in %).

Notation	Description	La Plata Basin			Amazon Basin			South America		
		wet	dry	year	wet	dry	year	wet	dry	year
ρ_{c}	Fraction of precip. originating from the continent	42 / 45	35 / 35	41 / 43	30 / 27	35 / 30	32 / 29	30 / 29	29 / 26	31 / 29
ρ_{Am}	Fraction of precip. originating from the AB through DMR	23 / 18	25 / 21	24 / 20	26 / 22	30 / 25	28 / 24	18 /15	21 / 18	20 / 17
ρ_{Am}^{casc}	Fraction of precip. originating from the AB through CMR	6 / 6	2 / 3	4 / 6	– / –	– /–	–/–	11 / 9	6 / 6	8 / 8
ε_{c}	Fraction of evap. that falls as precip. over the continent	43 / 40	16 / 16	35 / 32	77 / 68	45 / 41	65/57	56 / 29	31 / 28	47 / 42
ε_{Pl}	Fraction of evap. that falls as precip. over the LPB through DMR	32 / 28	12 / 11	26 / 22	16 / 11	7 / 6	11/10	15 / 13	7 / 6	12 / 11
ε_{Pl}^{casc}	Fraction of evap. that falls as precip. over the LPB through CMR	– / –	– / –	– / –	23 / 16	1 / 2	10 / 7	13 / 8	1 / 1	6 / 4
$\Delta P_{c}/P$	Fraction of precip. that comes from CMR on the continent	17 / 18	14 / 12	17 / 17	8 / 6	11 / 8	10 / 7	10 / 9	9 / 7	10 / 9
$\Delta P_{m}/P$	Fraction of precip. that comes from CMR in the intermediary region	8 / 10	4 / 3	6 / 7	4 / 3	6 / 4	5 /4	4 / 4	4 / 3	4 / 4
$\Delta E_{c}/E$	Fraction of evap. that lies within CMR pathways	11 / 13	9 / 8	9 /11	11 / 8	23 / 15	12 / 10	13 / 9	15 / 10	10 / 8

The fraction of precipitation in grid cell j that comes from Ω through CMR involving only one re-evaporation cycle is:

$$\rho_{\Omega,j}^{(1)} = \frac{\sum_{i \notin \Omega} m_{ji} \cdot \rho_{\Omega,i}}{P_j}, \tag{C3}$$

where ρ_{Ω_j} is the direct precipitation recycling ratio (Sect. C1.1). Following the same principle as in Eq. (C3), the fraction of precipitation in j that comes from Ω through CMR involving n re-evaporation cycles is:

$$\rho_{\Omega,j}^{(n)} = \frac{\sum_{i \notin \Omega} m_{ij} \cdot \rho_{\Omega,i}^{(n-1)}}{P_j}, \tag{C4}$$

where $\rho_{\Omega,i}^{(n-1)}$ is the fraction of precipitation in i that comes from Ω through CMR involving $n-1$ re-evaporation cycles. ρ_{Ω}^{casc} is the sum of all individual contributions of the CMR pathways:

$$\rho_{\Omega,j}^{casc} = \rho_{\Omega,j}^{(1)} + \ldots + \rho_{\Omega,j}^{(n)}. \tag{C5}$$

The fraction of evapotranspiration in grid cell i that falls as precipitation over Ω after only one re-evaporation cycle is:

$$\varepsilon_{\Omega,i}^{(1)} = \frac{\sum_{j \notin \Omega} m_{ij} \cdot \varepsilon_{\Omega,j}}{E_i}, \tag{C6}$$

where $\varepsilon_{\Omega,j}$ is the direct evapotranspiration recycling ratio (Sect. C1.1). Similarly, the fraction of evapotranspiration in i that falls as precipitation over Ω after n re-evaporation cycles is:

$$\varepsilon_{\Omega,i}^{(n)} = \frac{\sum_{j \notin \Omega} m_{ij} \cdot \varepsilon_{\Omega,j}^{(n-1)}}{E_i}, \tag{C7}$$

where $\varepsilon_{\Omega,j}^{(n-1)}$ is the fraction of evapotranspiration in j that precipitates over Ω after $n-1$ re-evaporation cycles. The $\varepsilon_{\Omega}^{casc}$ is the sum of the individual contribution of CMR pathways:

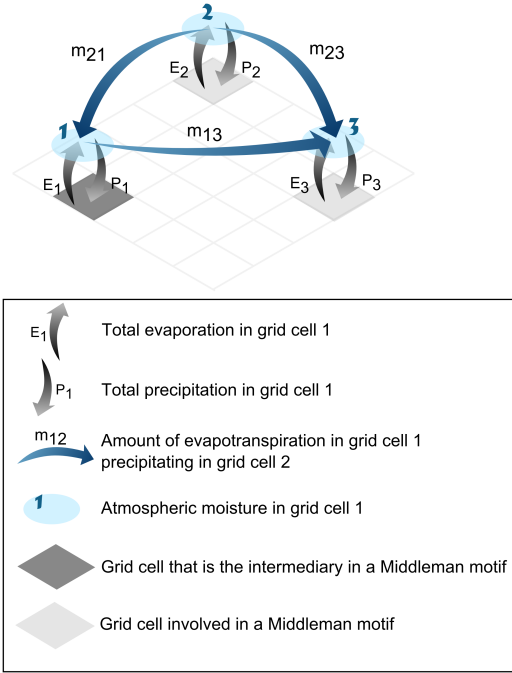$$\varepsilon_{\Omega,i}^{casc} = \varepsilon_{\Omega,i}^{(1)} + \ldots + \varepsilon_{\Omega,i}^{(n)} \tag{C8}$$

Fig. 3: Schematic representation of the Middleman motif from the perspective of grid cell 1. The grid cell 1 receives and distributes moisture from and to grid cells 2 and 3, which also exchange moisture such that there is no cyclic relation. The exchange of moisture between 2 and 3 uses two alternative pathways: the direct one (m_{23}) and the cascading pathway ($m_{21}m_{13}$). The grid cell 1 is an intermediary on an alternative pathway to the direct transport of moisture between 2 and 3.

C1.3   Robustness of the CMR (cascading moisture recycling) ratios

In order to test the robustness of the cascading precipitation recycling ratios, we have computed the steps explained in Sect. A1 and A2.1 with Ω being the ocean. Thus, ρ_o is the fraction of precipitation that comes from the ocean without any re-evaporation cycle on the way and $\rho_o^{(k)}$ is the fraction of precipitation that comes from the ocean with k re-evaporation cycle(s) on the way ($k = 1, ...n$). We confirm that:

– The sum $\rho_o + \rho_o^{(1)} + \rho_o^{(2)} + ... + \rho_o^{(n)}$ is equal to 1. This is easy to interpret as all the precipitation in a location must always have been come from the ocean (either directly or after a certain number of re-evaporation cycles).

– The sum $\rho_o^{(1)} + \rho_o^{(2)} + ... + \rho_o^{(n)}$ represents the fraction of precipitation that comes from the ocean with at least 1 re-evaporation cycle. It is equal to the continental recycling ratio ρ_c (see Sect. 2.3.1 and van der Ent et al. (2010)).

– The sum $\rho_o^{(2)} + ... + \rho_o^{(n)}$ is the fraction of precipitation that comes from the ocean with at least 2 re-evaporation cycles. It is equal to $\Delta P/P$, introduced as the fraction precipitation that has been evaporated at least twice on the continent (see Sect. 2.4).

We obtained thus the same results using different metrics. We can't test the evaporation recycling ratio the same way because $\Delta E/E$ quantifies the fraction of evapotranspiration that is involved in cascading moisture recycling (i.e., that comes from the continent and precipitates further over the continent) while $\epsilon_o^{(2)} + ... + \epsilon_o^{(n)}$ would be the fraction of evapotranspiration that runs through at least 2 re-evaporation cycles before precipitating over the ocean. This is also the reason why the two methodologies are needed even if they lead to the same results for the previous mentioned case.

C2   Quantifying CMR (cascading moisture recycling)

To quantify the contribution of CMR to total moisture in- and outflow, we cut-off all re-evaporation of moisture from continental origin. By doing so, we inhibit all cascading recycling of moisture from continental origin in the network (see Fig. B1). To achieve this, we derive for each grid cell the evaporation of moisture from oceanic origin (i.e., that has been last evaporated over the ocean) as in Eq. (1):

$$E_{i \leftarrow \text{ocean}} = \frac{E_i}{P_i} \cdot P_{i \leftarrow \text{ocean}}, \tag{C9}$$

where $P_{i \leftarrow \text{ocean}}$ is the precipitation from oceanic origin in i ($P_{j \leftarrow \text{ocean}} = P_j - P_{j \leftarrow \text{continent}}$ and $P_{j \leftarrow \text{continent}} = \sum_{i \in \text{continent}} m_{ij}$.). Using the same assumption, we get the moisture transport between each pair of grid cells i and j that results from evaporation of moisture from oceanic origin only:

$$m_{ij \leftarrow \text{ocean}} = \frac{m_{ij}}{E_i} \cdot E_{i \leftarrow \text{ocean}}, \tag{C10}$$

At this stage, $m_{ij \leftarrow \text{ocean}}$ can be interpreted as the evapotranspiration in i that precipitates in j and that has been evaporated from the ocean before that ($m_{ij \leftarrow \text{ocean}} < m_{ij}$).

In a second step, we derive the corresponding moisture in- and outflow from or towards a given region Ω for each grid cell:

$$P_{j \leftarrow \Omega, o} = \sum_{i \in \Omega} m_{ij \leftarrow \text{ocean}} \tag{C11a}$$

$$E_{i \rightarrow \Omega, o} = \sum_{j \in \Omega} m_{ij \leftarrow \text{ocean}}. \tag{C11b}$$

Dry season

(a) Precip. (b) Evap. (c) Evap. - Precip. (d) ρ_c (e) ε_c

Wet season

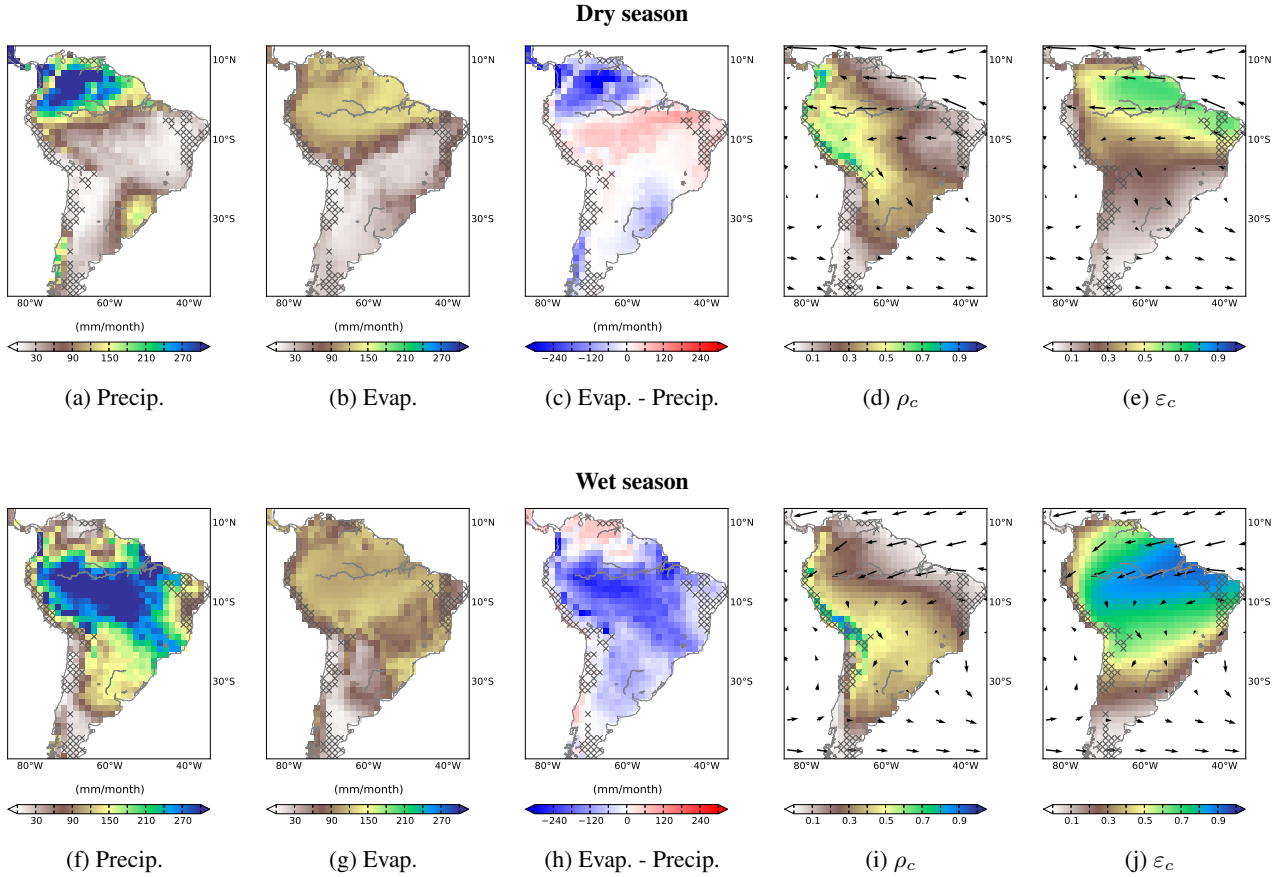(f) Precip. (g) Evap. (h) Evap. - Precip. (i) ρ_c (j) ε_c

Fig. 4: WAM-2layers input and output as calculated for the period 2001 – 2010 for MODIS and TRMM (input MOD, see Table 1): long term seasonal mean of precipitation **(a, f)**, evapotranspiration **(b, g)**, precipitation – evapotranspiration **(c, h)**, continental precipitation recycling ratio ρ_c **(d, i)** and continental evapotranspiration recycling ratio ε_c **(e, j)** indicating respective sinks and sources of continental moisture. Here and in the following figures, the vectors indicate the horizontal moisture flux field (in m^3 of moisture $\times$ m^{-2} $\times$ month^{-1}) and the hatches represent grid cells where annual mean evapotranspiration exceeds mean annual precipitation. Results are given for the dry season (JJAS) (upper row) and the wet season (DJFM) (lower row).

$P_{j\leftarrow\Omega,o}$ can be interpreted as the precipitation in j originating from the re-evaporation of oceanic moisture in Ω. Similarly, $E_{i\rightarrow\Omega,o}$ can be seen as the evapotranspiration of oceanic moisture in i that precipitates over Ω.

Thus, are able to derive the corresponding reduction in total moisture inflow towards Ω or outflow from Ω:

$$\Delta P_{j\leftarrow\Omega} = P_{j\leftarrow\Omega} - P_{j\leftarrow\Omega,o} \quad \text{(C12a)}$$
$$\Delta E_{i\rightarrow\Omega} = E_{i\rightarrow\Omega} - E_{i\rightarrow\Omega,o}, \quad \text{(C12b)}$$

where $P_{j\leftarrow\Omega} = \sum_{i\in\Omega} m_{ij}$ is the total precipitation in j originating from Ω and $E_{j\rightarrow\Omega} = \sum_{j\in\Omega} m_{ij}$ is the total evapotranspiration in i that contributes to precipitation over Ω. Thus, $\Delta P_{j\leftarrow\Omega}$ is the precipitation in j originating from the re-evaporation of continental moisture in Ω and $\Delta E_{i\rightarrow\Omega}$ is the re-evaporation of continental moisture in i that precipitates over Ω.

If Ω is the entire South American continent (resp. the intermediary region), $\Delta P_{j\leftarrow\Omega}$ becomes $\boldsymbol{\Delta P_c}$ (resp. $\boldsymbol{\Delta P_m}$) and $\Delta E_{i\rightarrow\Omega}$ becomes $\boldsymbol{\Delta E_c}$ (resp. $\boldsymbol{\Delta E_m}$) as defined in Sect. 2.4.

C3 Complex network analysis

C3.1 Clustering coefficient associated with Middleman motifs

Mathematically, the clustering coefficient C of the grid cell i is:

$$C_i = \frac{t_i}{T_i}, \quad \text{(C13)}$$

where t_i is the number of Middleman motifs that i forms and T_i is the total number of that motif that i could have formed according to its number of incoming and outgoing arrows. To give more weight to a motif involved in the transport of a larger amount of moisture, we assign a weight to each mo-

Dry season

(a) Precip.   (b) Evap.   (c) Evap. - Precip.   (d) ρ_c (e) ε_c

Wet season

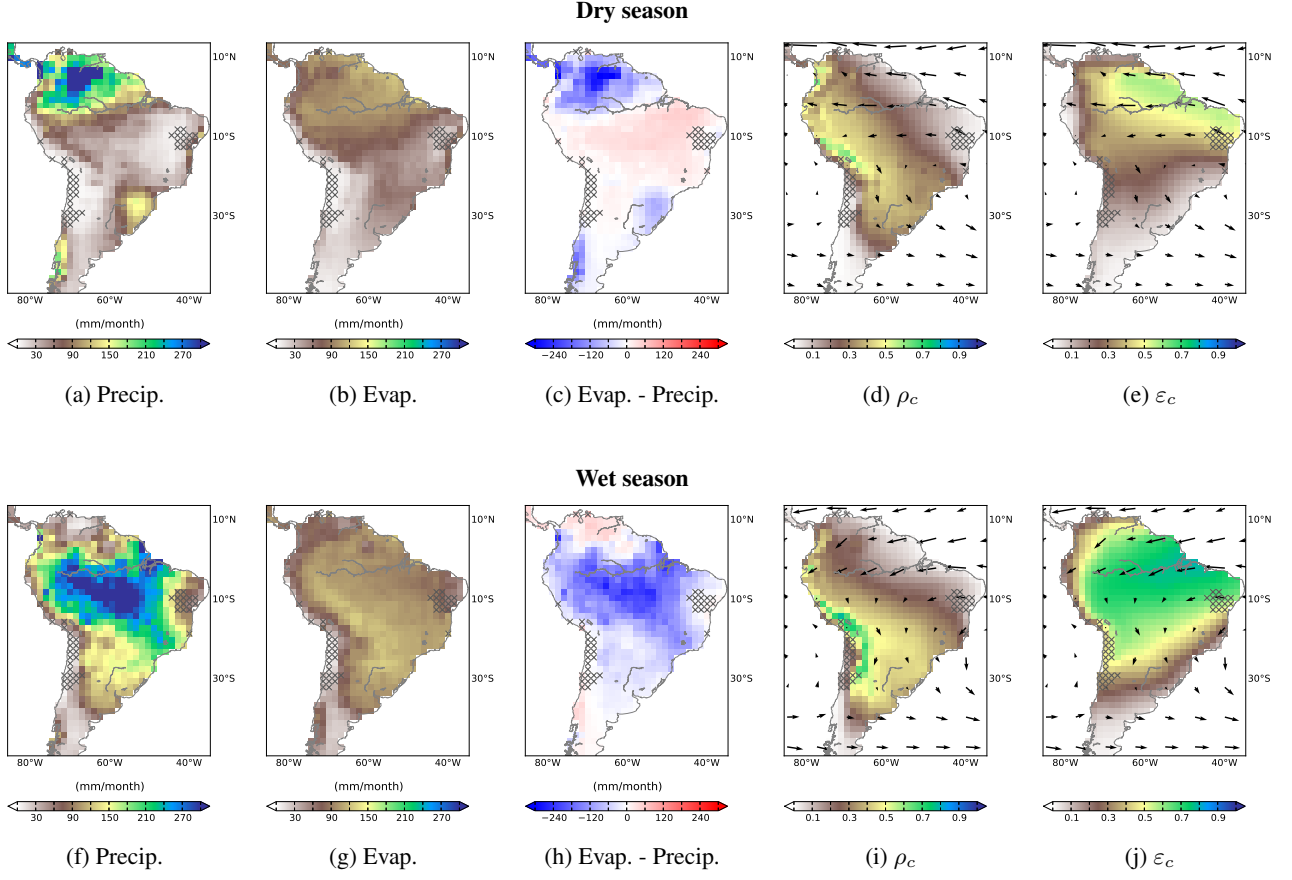(f) Precip.   (g) Evap.   (h) Evap. - Precip.   (i) ρ_c (j) ε_c

Fig. 5: Same as Fig. 4 for the period 1990–1995 as calculated from LandFluxEval and an average of four observation-based precipitation products (input LFE, see Table 1).

tif. In agreement with Fagiolo (2007), the weight of a motif is defined as the geometric mean of the weights of the three involved arrows. The weighted counterpart of Eq. (C13) is:

$$\tilde{C}_i = \frac{\tilde{t}_i}{T_i}, \tag{C14}$$

with $\tilde{t}_i$ the weighted counterpart of t_i (i.e., the sum of the weights of the Middleman motifs that is formed by i).

The calculation of the clustering coefficient is derived from the methodology of a previous study (Fagiolo, 2007, Table 1) and has been corrected in order to account for the irregular sizes of the portion of the Earth's surface covered by the grid cells as explained in Zemp et al. (2014). The numerator of Eq. (C14) can be derived as $\tilde{t}_i = (\mathbf{P}\mathbf{P}^{\mathrm{T}}\mathbf{P})_{ii}$ with $\mathbf{P} = \{p_{ij}^{1/3}\}_{i,j \in N}$ and p_{ij} is the weight of the arrow originating from i and pointing towards j. Here, in order to avoid a strong correlation between the clustering coefficient and the mean evapotranspiration and precipitation, we chose this weight to be $p_{ij} = m_{ij}^2/(E_i P_j)$. The denominator of Eq. (C14) is $T_i = k_i^{\mathrm{in}} k_i^{\mathrm{out}}$ where k_i^{in} is the number of arrows pointing towards i and k_i^{out} the number of arrows originating

from i:

$$k_i^{\mathrm{in}} = \sum_{j \neq i} a_{ji}, \tag{C15a}$$

$$k_i^{\mathrm{out}} = \sum_{j \neq i} a_{ij}, \tag{C15b}$$

where $a_{ij} = 1$ if there is an arrow originating from i and pointing towards j and $a_{ij} = 0$ otherwise. In order to compare the results for the two seasons, we normalize $\tilde{C}$ with the maximum observed value for each network.

C3.2   Optimal pathway

In complex network theory, many centrality measures (e.g. closeness and betweenness) are based on the concept of a shortest path. The shortest path is usually defined as the pathway between nodes that has the minimum cost. In this work, it is defined as the pathway that contributes most to the moisture transport between two grid cells. As this pathway is not necessarily the shortest one in term of geographical distance, we will call it "optimal pathway" to avoid confusion.
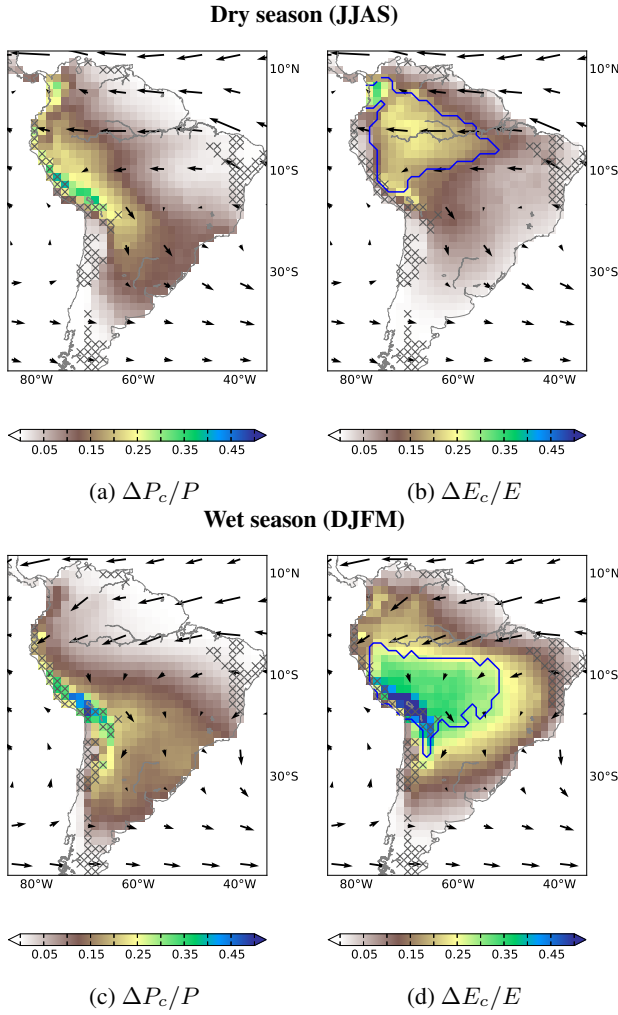
Dry season (JJAS)

(a) $\Delta P_c/P$ (b) $\Delta E_c/E$

Wet season (DJFM)

(c) $\Delta P_c/P$ (d) $\Delta E_c/E$

Fig. 6: Fraction of total precipitation originating from CMR ($\Delta P_c/P$) **(a, c)** and fraction of total evapotranspiration that lies within CMR pathways ($\Delta E_c/E$) **(b, d)**. While high values of $\Delta P_c/P$ indicate regions that are dependent on CMR for local rainfall, high values of $\Delta E_c/E$ indicate regions that contribute to CMR. The blue boundaries define the intermediary regions ($\Delta E_c/E > 80\% il$ calculated for all seasonal values over the continent). Results are obtained using the input MOD (see Table 1) and are given for the dry season (JJAS) (upper row) and the wet season (DJFM) (lower row).

Dry season (JJAS)

(a) $\tilde{C}$ (b) B

Wet season (DJFM)

(c) $\tilde{C}$ (d) B

Fig. 7: Complex network analysis. Clustering coefficient $\tilde{C}$ associated with the motif Middleman **(a, c)** and betweenness centrality B **(b, d)**. While high values of $\tilde{C}$ indicate intermediary locations where CMR allows for alternative pathways to the direct transport of moisture, high values of B indicate regions where pathways of CMR are channeled. Results are obtained using the input MOD (see Table 1) and are given for the dry season (JJAS) (upper row) and the wet season (DJFM) (lower row).

Let $(t_1, t_2, \ldots, t_n)$ be the intermediary grid cells in a CMR pathway from grid cell i to grid cell j. The contribution of this pathway is defined as the fraction of precipitation in j that comes from evapotranspiration in i through CMR:

$$W_{i,t_1,\ldots,t_n,j} = \frac{m_{it_1}}{P_{t_1}} \cdot \prod_{l=1}^{n-1} \frac{m_{t_l t_{l+1}}}{P_{t_{l+1}}} \cdot \frac{m_{t_n j}}{P_j} \qquad \text{(C16)}$$

An example of pathway contributions is provided in Fig. B1. The contribution of each existing pathway is calculated be-

tween any pair of grid cells in the network. The optimal pathway is the path with the maximum contribution.
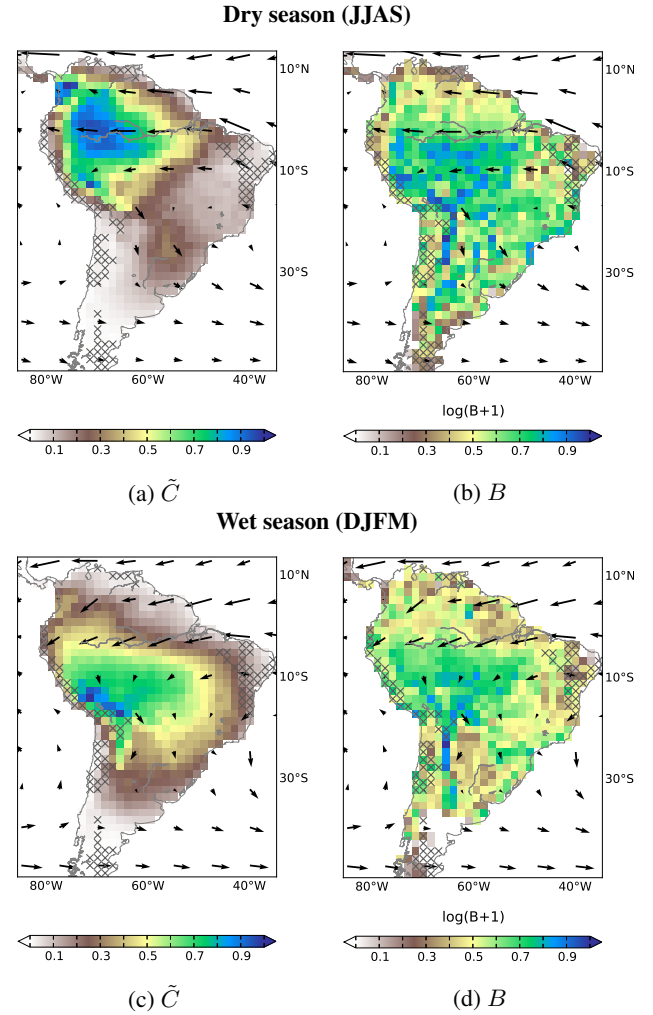
To find the optimal pathway, we use the method `shortest_paths` in the package iGraph for Python based on an algorithm proposed by Newman (2001). In this method, the cost of a pathway is calculated as the sum of the weight of its arrows. In order to adapt the method to our purpose, we chose the weight of the arrows as $w_{t_l t_{l+1}} = -\log\left(\frac{m_{t_l t_{l+1}}}{P_{t_{l+1}}}\right)$. The cost of a pathway from grid cell i to
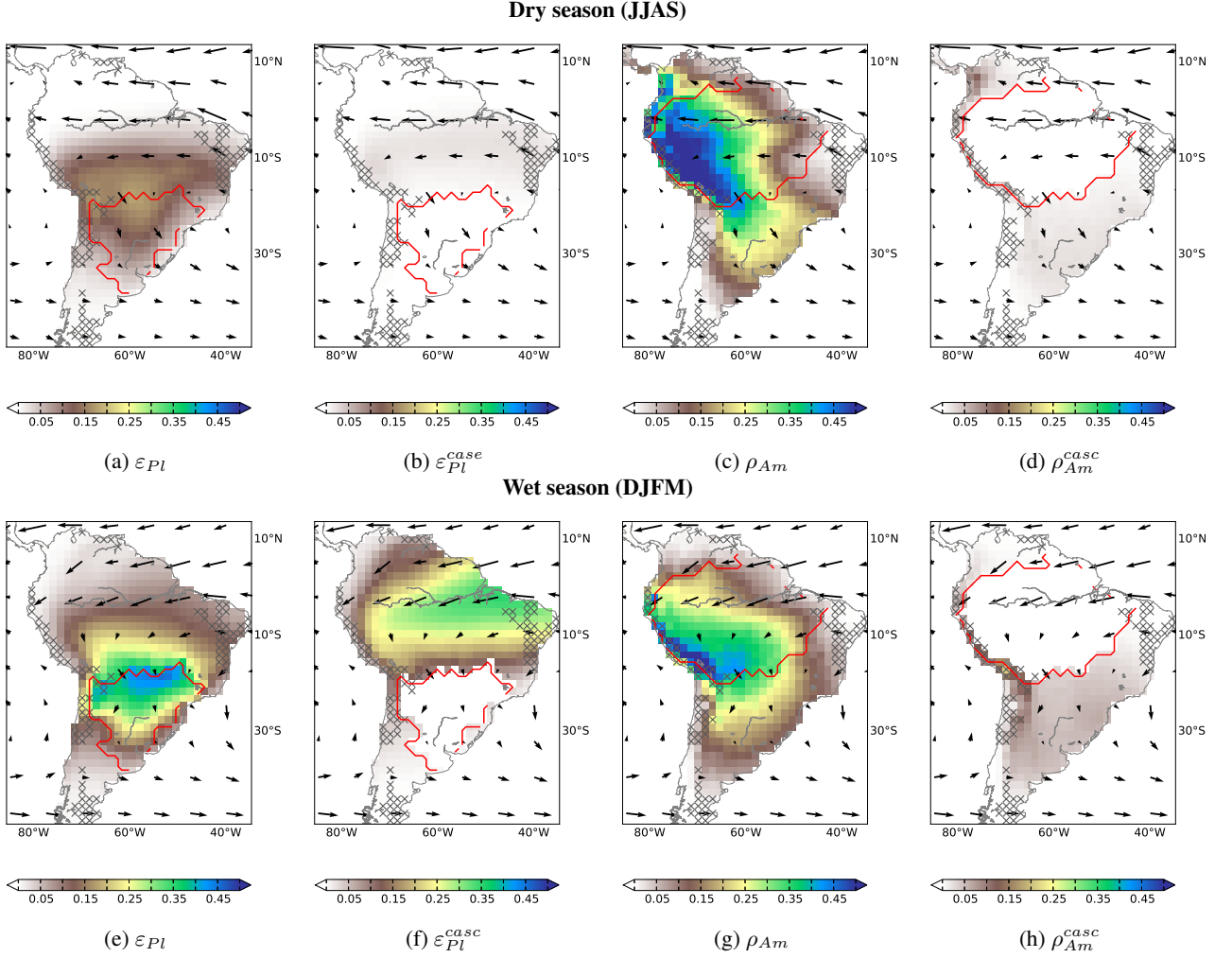
Dry season (JJAS)

(a) ε_{Pl} (b) ε_{Pl}^{casc} (c) ρ_{Am} (d) ρ_{Am}^{casc}

Wet season (DJFM)

(e) ε_{Pl} (f) ε_{Pl}^{casc} (g) ρ_{Am} (h) ρ_{Am}^{casc}

Fig. 8: Fraction of evapotranspiration that precipitates over the La Plata basin (defined by the red boundaries) through DMR (ε_{Pl}, **a** and **e**) and CMR (ε_{Pl}^{casc}, **b** and **f**) and fraction of precipitation that comes from the Amazon basin (defined by the red boundaries) through DMR (ρ_{Am}, **c** and **g**) and CMR (ρ_{Am}^{casc}, **d** and **h**). Considered together, ε_{Pl} and ε_{Pl}^{casc} show source regions of precipitation over the La Plata basin and ρ_{Am} and ρ_{Am}^{casc} show sink regions of evapotranspiration from the La Plata basin. Results are obtained using the input MOD (see Table 1) and are given for the dry season (JJAS) (upper row) and the wet season (DJFM) (lower row).

grid cell j as calculated in iGraph becomes:

$$
\begin{aligned}
W'_{i,t_1,\dots,t_n,j} &= w_{1t_1} + \sum_{l=1}^{n-1} w_{t_l t_{l+1}} + w_{t_n j} \\
&= -\log\left(\frac{m_{it_1}}{P_{t_1}}\right) - \sum_{l=1}^{n-1} \log\left(\frac{m_{t_l t_{l+1}}}{P_{t_{l+1}}}\right) \\
&\quad - \log\left(\frac{m_{t_n j}}{P_j}\right) \\
&= \log\left(\frac{1}{\frac{m_{1t_1}}{P_{t_1}} \cdot \prod_{l=1}^{n-1}\left(\frac{m_{t_l t_{l+1}}}{P_{t_{l+1}}}\right) \cdot \frac{m_{t_n j}}{P_j}}\right) \\
&= \log\left(\frac{1}{W_{i,t_1,\dots,t_n,j}}\right)
\end{aligned}
$$

Because the optimal pathway is defined as the pathway with the minimum cost W', it corresponds to the pathway with the maximum contribution W as defined above.

C3.3   Betweenness centrality

Mathematically, betweenness of the grid cell i is the fraction of the number of optimal pathways between any pair of grid cells that pass through i:

$$
B_i = \sum_{j,k} \frac{\sigma_{jk}(i)}{\sigma_{jk}} \tag{C17}
$$

with σ_{jk} is the number of optimal pathways between grid cells j and k, and $\sigma_{jk}(i)$ is the number of these pathways

Dry season (JJAS)

(a) $\Delta P_c/P$

(b) $\Delta E_c/E$

Wet season (DJFM)

(c) $\Delta P_c/P$
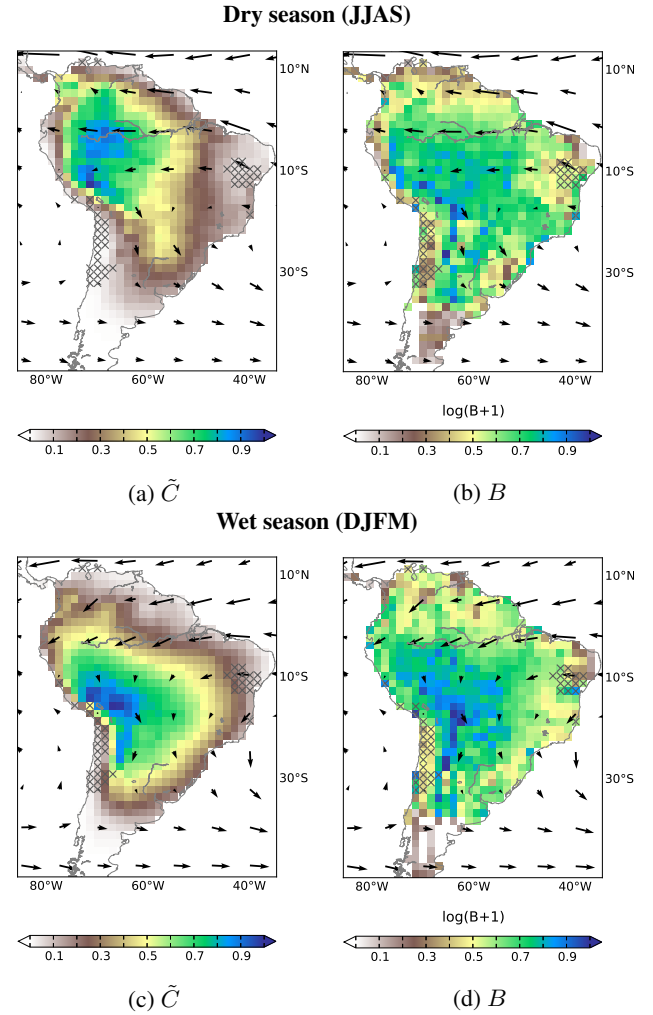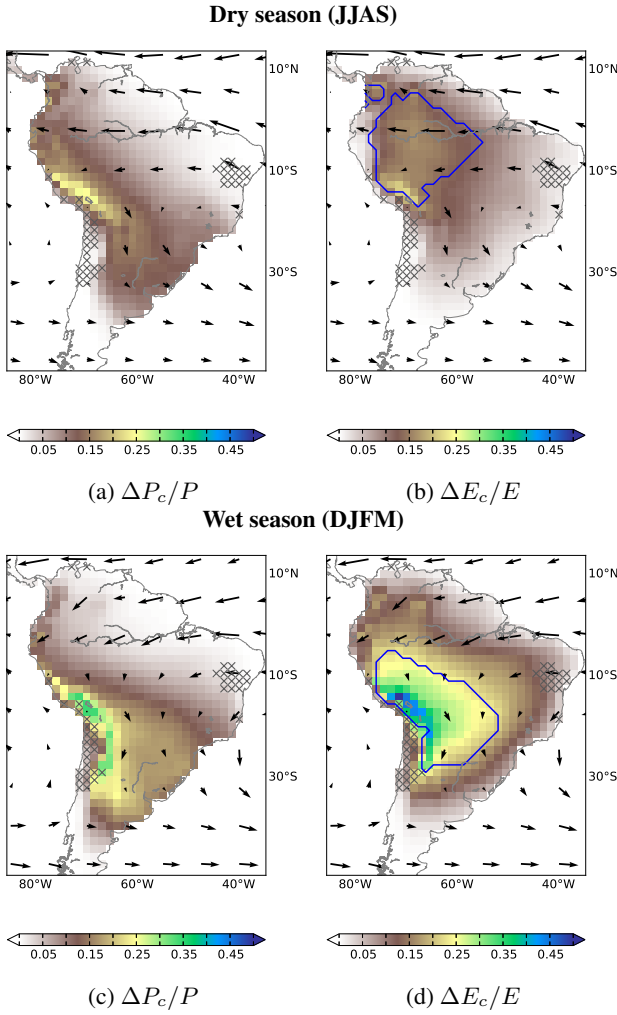
(d) $\Delta E_c/E$

Fig. B1: Fraction of total precipitation originating from CMR ($\Delta P_c/P$) **(a, c)** and fraction of total evapotranspiration that lies within CMR pathways ($\Delta E_c/E$) **(b, d)**. While high values of $\Delta P_c/P$ indicate regions that are dependent on CMR for local rainfall, high values of $\Delta E_c/E$ indicate regions that contribute to CMR. The blue boundaries define the intermediary regions ($\Delta E_c/E > 80\% il$ calculated for all seasonal values over the continent). Results are obtained using the input LFE (see Table 1) and are given for the dry season (JJAS) (upper row) and the wet season (DJFM) (lower row).

Dry season (JJAS)

(a) $\tilde{C}$

(b) B

Wet season (DJFM)

(c) $\tilde{C}$

(d) B

Fig. B2: Complex network analysis. Clustering coefficient $\tilde{C}$ associated with the motif Middleman **(a, c)** and betweenness centrality B **(b, d)**. While high values of $\tilde{C}$ indicate intermediary locations where CMR allows for alternative pathways to the direct transport of moisture, high values of B indicate regions where pathways of CMR are channeled. Results are obtained using the input LFE (see Table 1) and are given for the dry season (JJAS) (upper row) and the wet season (DJFM) (lower row).

that pass through the grid cell i. B reaches values between 0 and $\binom{N-1}{2} = (N^2 - 3N + 2)/2$ with N the number of grid cells. To calculate it, we used the directed and weighted version of the method `betweenness` in the package iGraph for Python. The choice of the weights used in this method is explained in Sect. C3.2.

Author contribution

Dry season (JJAS)

(a) ε_{Pl} (b) ε_{Pl}^{case} (c) ρ_{Am} (d) ρ_{Am}^{casc}

Wet season (DJFM)

(e) ε_{Pl} (f) ε_{Pl}^{casc} (g) ρ_{Am} (h) ρ_{Am}^{casc}
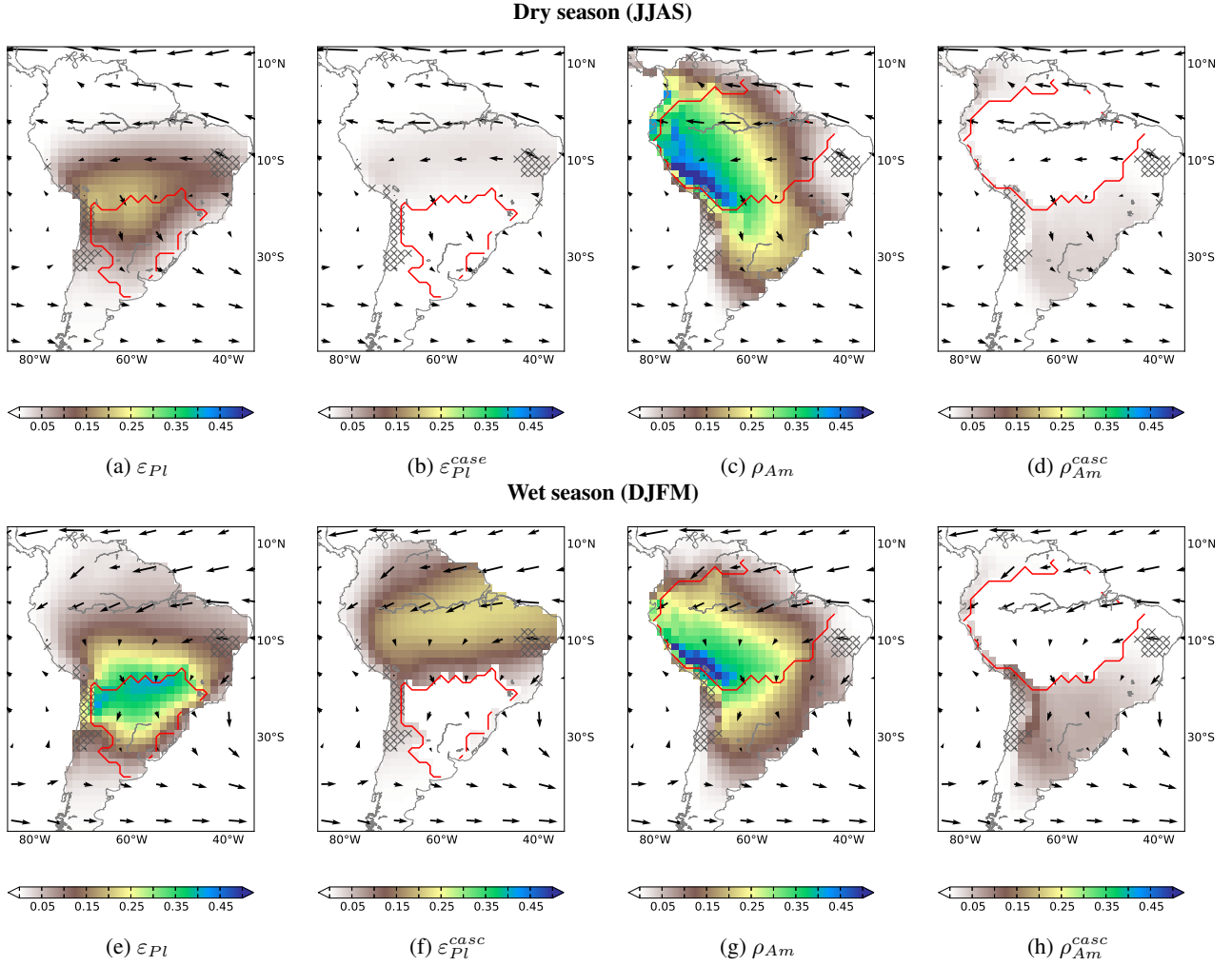
Fig. B3: Fraction of evapotranspiration that precipitates over the La Plata basin (defined by the red boundaries) through DMR (ε_{Pl}, **a** and **e**) and CMR (ε_{Pl}^{casc}, **b** and **f**) and fraction of precipitation that comes from the Amazon basin (defined by the red boundaries) through DMR (ρ_{Am}, **c** and **g**) and CMR (ρ_{Am}^{casc}, **d** and **h**). Considered together, ε_{Pl} and ε_{Pl}^{casc} show source regions of precipitation over the La Plata basin and ρ_{Am} and ρ_{Am}^{casc} show sink regions of evapotranspiration from the La Plata basin. Results are obtained using the input LFE (see Table 1) and are given for the dry season (JJAS) (upper row) and the wet season (DJFM) (lower row).

References

Adler, R. F., Huffman, G. J., Chang, A., Ferraro, R., Xie, P. P., Janowiak, J., Rudolf, B., Schneider, U., Curtis, S., Bolvin, D., Gruber, A., Susskind, J., Arkin, P., and Nelkin, E.: The version-2 global precipitation climatology project (GPCP) monthly precipitation analysis (1979–present), J. Hydrometeorol., 4, 1147–1167, 2003.

Arraut, J. M. and Satyamurty, P.: Precipitation and water vapor transport in the Southern Hemisphere with emphasis on the South American region, J. Appl. Meteorol. Clim., 48, 1902–1912, 2009.

Arraut, J. M., Nobre, C., Barbosa, H. M., Obregon, G., and Marengo, J.: Aerial rivers and lakes: looking at large-scale moisture transport and its relation to Amazonia and to subtropical
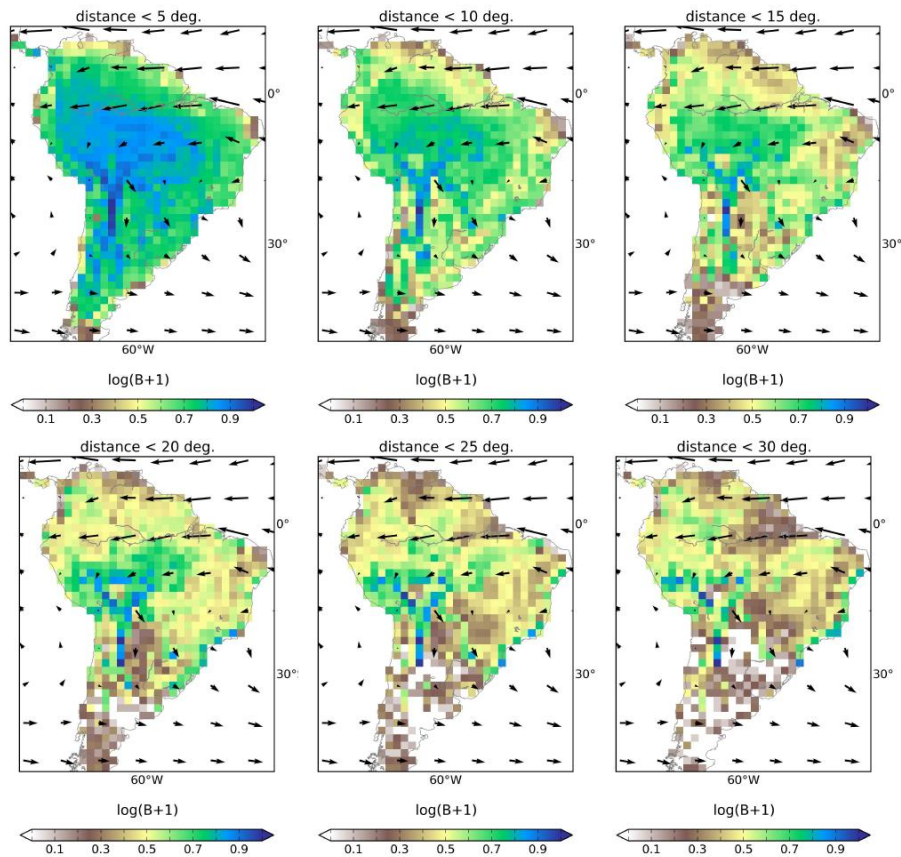
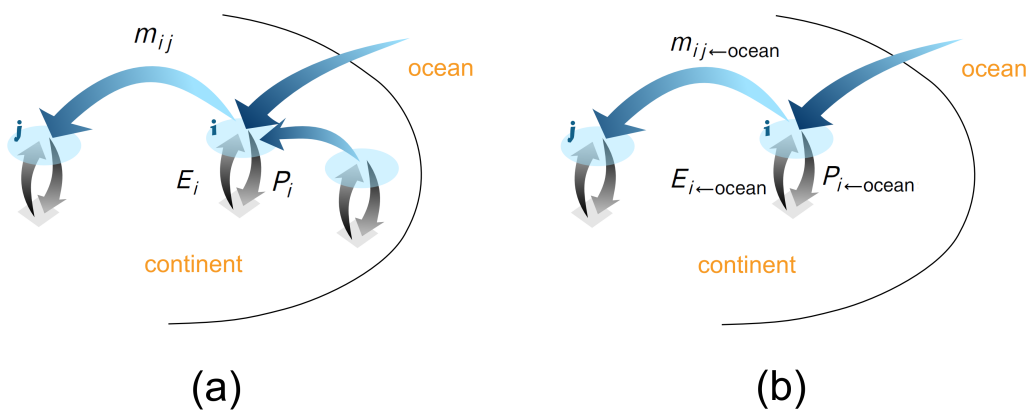Fig. B4: Betweenness Centrality (B) obtained for different thresholds (yearly average for the input MOD).

(a)   (b)

Fig. C1: Scheme explaining the removal of CMR. Originally, the precipitation in the grid cell i (P_i) is composed by oceanic and continental moisture. The total incoming moisture is evaporated in i (E_i) and some part of it contributes to precipitation in the grid cell j (m_{ij}) (a). If we forbid the re-evaporation of continental precipitation, only the precipitation in i that has oceanic origin ($P_{i\leftarrow\text{ocean}}$) is evaporated in i ($E_{i\leftarrow\text{ocean}}$) and can contribute to precipitation in j ($m_{ij\leftarrow\text{ocean}}$). By doing so, we remove cascading recycling of continental moisture from the network (b).
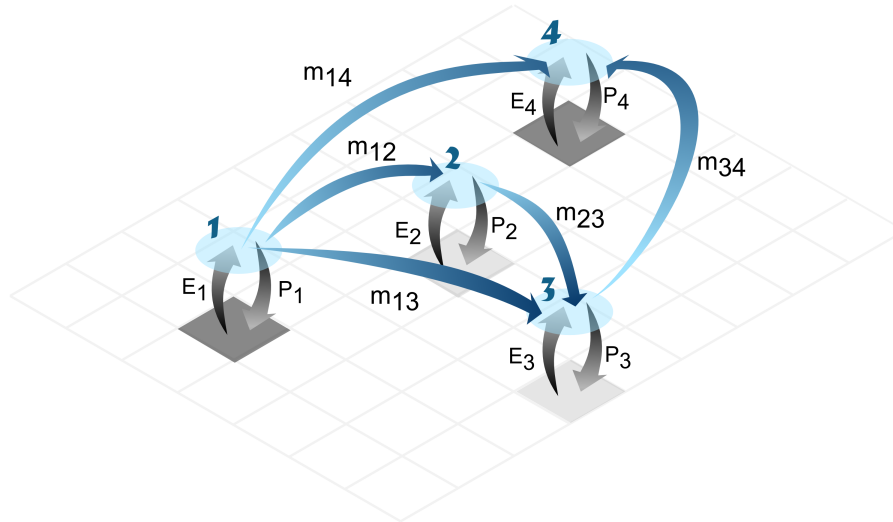
Fig. C2: Different CMR pathways from grid cell 1 to grid cell 4. The contribution of the direct pathway is $W_{1,4} = m_{14}/P4$, the contribution of the path involving one re-evaporation cycle in grid cell 3 is $W_{1,3,4} = m_{13}/P3 \cdot m_{14}/P4$ and the contribution of the path involving re-evaporation cycles in grid cells 2 and 3 is $W_{1,2,3,4} = m_{12}/P2 \cdot m_{13}/P3 \cdot m_{14}/P4$. The legend is the same that in Fig. 1.

rainfall in South America, J. Climate, 25, 543–556, 2012.

Bagley, J. E., Desai, A. R., Harding, K. J., Snyder, P. K., and Foley, J. A.: Drought and deforestation: has land cover change influenced recent precipitation extremes in the Amazon?, J. Climate, 27, 345–361, 2014.

Betts, R., Cox, P., Collins, M., Harris, P., Huntingford, C., and Jones, C.: The role of ecosystem-atmosphere interactions in simulated Amazonian precipitation decrease and forest dieback under global climate warming, Theor. Appl. Climatol., 78, 157–175, 2004.

Boers, N., Bookhagen, B., Marwan, N., Kurths, J., and Marengo, J.: Complex networks identify spatial patterns of extreme rainfall events of the South American Monsoon System, Geophys. Res. Lett., 40, 4386–4392, 2013.

Bosilovich, M. G. and Chern, J.-D.: Simulation of water sources and precipitation recycling for the MacKenzie, Mississippi, and Amazon River basins, J. Hydrometeorol., 7, 312–329, 2006.

Brubaker, K. L., Entekhabi, D., and Eagleson, P. S.: Estimation of continental precipitation recycling, J. Climate, 6, 1077–1089, 1993.

Burde, G. I. and Zangvil, A.: The estimation of regional precipitation recycling. Part I: Review of recycling models, J. Climate, 14, 2497–2508, 2001.

Burde, G. I., Gandush, C., and Bayarjargal, Y.: Bulk recycling models with incomplete vertical mixing. Part II: Precipitation recycling in the Amazon basin, J. Climate, 19, 1473–1489, 2006.

Chen, M. Y., Shi, W., Xie, P. P., Silva, V. B. S., Kousky, V. E., Higgins, R.W., and Janowiak, J. E.: Assessing objective techniques for gauge-based analyses of global daily precipitation, J. Geophys. Res.-Atmos., 113, D04110, 2008.

Costa, M. H., Biajoli, M. C., Sanches, L., Malhado, A. C. M., Hutyra, L. R., da Rocha, H. R., Aguiar, R. G., and de Araújo, A. C.: Atmospheric versus vegetation controls of Amazonian tropical rain forest evapotranspiration: are the wet and seasonally dry rain forests any different?, J. Geophys. Res.-Biogeo., 115, G0402, doi:10.1029/2009JG001179, 2010.

Cox, P. M., Betts, R. A., Collins, M., Harris, P. P., Huntingford, C., and Jones, C. D.: Amazonian forest dieback under climate-carbon cycle projections for the 21st century, Theor. Appl. Climatol., 78, 137–156, 2004.

Da Silva, R. R., Werth, D., and Avissar, R.: Regional impacts of future land-cover changes on the Amazon basin wet-season climate, J. Climate, 21, 1153–1170, 2008.

Dee, D. and Uppala, S.: Variational bias correction in ERA-Interim, no. 575 in Technical Memorandum, ECMWF, Shinfield Park, Reading, England, 2008.

Dee, D. P., Uppala, S. M., Simmons, A. J., Berrisford, P., Poli, P., Kobayashi, S., Andrae, U., Balmaseda, M. A., Balsamo, G., Bauer, P., Bechtold, P., Beljaars, A. C. M., van de Berg, L., Bidlot, J., Bormann, N., Delsol, C., Dragani, R., Fuentes, M., Geer, A. J., Haimberger, L., Healy, S. B., Hersbach, H., Hólm, E. V., Isaksen, L., Kållberg, P., Köhler, M., Matricardi, M., McNally, A. P., Monge-Sanz, B. M., Morcrette, J.-J., Park, B.-K., Peubey, C., de Rosnay, P., Tavolato, C., Thépaut, J.-N., and Vitart, F.: The ERA-Interim reanalysis: configuration and performance of the data assimilation system, Q. J. Roy. Meteor. Soc., 137, 553–597, 2011.

Dirmeyer, P. A., Brubaker, K. L., and DelSole, T.: Import and export of atmospheric water vapor between nations, J. Hydrol., 365, 11–22, 2009.

Donges, J. F., Zou, Y., Marwan, N., and Kurths, J.: Complex networks in climate dynamics – Comparing linear and nonlinear network construction methods, Eur. Phys. J.-Spec. Top., 174, 157–179, 2009a.

Donges, J. F., Zou, Y., Marwan, N., and Kurths, J.: The backbone of the climate network, Europhys. Lett., 87, 48007, doi:10.1209/0295-5075/87/48007, 2009b.

Drumond, A., Nieto, R., Gimeno, L., and Ambrizzi, T.: A Lagrangian identification of major sources of moisture over Central Brazil and La Plata basin, J. Geophys. Res., 113, D14128, doi:10.1029/2007JD009547, 2008.

Drumond, A., Marengo, J., Ambrizzi, T., Nieto, R., Moreira, L., and Gimeno, L.: The role of Amazon basin moisture on the atmospheric branch of the hydrological cycle: a Lagrangian analysis, Hydrol. Earth Syst. Sci. Discuss., 11, 1023–1046, doi:10.5194/hessd-11-1023-2014, 2014.

Eltahir, E. A. B. and Bras, R. L.: Precipitation recycling in the Amazon basin, Q. J. Roy. Meteor. Soc., 120, 861–880, 1994.

Fagiolo, G.: Clustering in complex directed networks, Phys. Rev. E, 76, 026107, doi:10.1103/PhysRevE.76.026107, 2007.

Figueroa, S. N. and Nobre, C. A.: Precipitation distribution over central and western tropical South America, Climanalise, 5, 36–45, 1990.

Franchito, S. H., Rao, V. B., Vasques, A. C., Santo, C. M. E., and Conforte, J. C.: Validation of TRMM precipitation radar monthly rainfall estimates over Brazil, J. Geophys. Res.-Atmos., 114, D02105, doi:10.1029/2007JD009580, 2009.

Freeman, L. C.: A set of measures of centrality based on betweenness, Sociometry, 40, 35–41, 1977.

Gat, J. and Matsui, E.: Atmospheric water balance in the Amazon basin: an isotopic evapotranspiration model, J. Geophys. Res.-Atmos., 96, 13179–13188, 1991.

Goessling, H. F. and Reick, C. H.: Continental moisture recycling as a Poisson process, Hydrol. Earth Syst. Sci., 17, 4133–4142, doi:10.5194/hess-17-4133-2013, 2013.

Grimm, A. M., Vera, C. S., and Mechoso, C. R.: The South American Monsoon System, in: The Third International Workshop on Monsoons, World Meteorological Organizations, Hangzhou, 111–129, 2–6 November 2004.

Hasler, N., Werth, D., and Avissar, R.: Effects of tropical deforestation on global hydroclimate: a multimodel ensemble analysis, J. Climate, 22, 1124–1141, 2009.

Hirota, M., Holmgren, M., Van Nes, E. H., and Scheffer, M.: Global resilience of tropical forest and savanna to critical transitions, Science, 334, 232–235, 2011.

Huffman, G. J., Adler, R. F., Rudolf, B., Schneider, U., and Keehn, P. R.: Global precipitation estimates based on a technique for combining satellite-based estimates, rain-gauge analysis and NWP model precipitation information, J. Climate, 8, 1284–1295, 1995.

Huffman, G. J., Adler, R. F., Bolvin, D. T., Gu, G., Nelkin, E. J., Bowman, K. P., Hong, Y., Stocker, E. F., and Wolff, D. B.: The TRMM Multisatellite Precipitation Analysis (TMPA): quasi-global, multiyear, combined-sensor precipitation estimates at fine scales, J. Hydrometeorol., 8, 38–55, 2007.

Keys, P. W., van der Ent, R. J., Gordon, L. J., Hoff, H., Nikoli, R., and Savenije, H. H. G.: Analyzing precipitationsheds to understand the vulnerability of rainfall dependent regions, Biogeosciences, 9, 733–746, doi:10.5194/bg-9-733-2012, 2012.

Keys, P. W. and Barnes, E. A. and van der Ent, R. J. and Gordon, L. J.: Variability of moisture recycling using a precipitationshed framework, Hydrol. Earth Syst. Sci. Discuss., 11, 5143–5178, doi:10.5194/hessd-11-5143-2014, 2014.

Kim, J.-E. and Alexander, M. J.: Tropical precipitation variability and convectively coupled equatorial waves on submonthly time scales in reanalyses and TRMM, J. Climate, 26, 3013–3030, 2013.

Knox, R., Bisht, G., Wang, J., and Bras, R.: Precipitation variability over the forest-to-nonforest transition in southwestern Amazonia, J. Climate, 24, 2368–2377, 2011.

Lean, J. and Warrilow, D. A.: Simulation of the regional climatic impact of Amazon deforestation, Nature, 342, 411–413, 1989.

Lewis, S. L., Brando, P. M., Phillips, O. L., van der Heijden, G. M., and Nepstad, D.: The 2010 amazon drought, Science, 331, 554–554, 2011.

Liebman, B., Kiladis, G. N., Marengo, J. A., Ambrizzi, T., and Glick, J. D.: Submonthly convective variability over South America and the South Atlantic convergence zone, J. Climate, 12, 1877–1891, 1999.

Loarie, S. R., Lobell, D. B., Asner, G. P., Mu, Q., and Field, C. B.: Direct impacts on local climate of sugar-cane expansion in Brazil, Nature Climate Change, 1, 105–109, 2011.

Ludescher, J., Gozolchiani, A., Bogachev, M. I., Bunde, A., Havlin, S., Schellnhuber, H. J.: Improved El Niño forecasting by cooperativity detection, P. Natl. Acad. Sci. USA, 110, 11742–11745, 2013.

Malik, N., Bookhagen, B., Marwan, N., and Kurths, J.: Analysis of spatial and temporal extreme monsoonal rainfall over South Asia using complex networks, Clim. Dynam., 39, 971–987, 2012.

Marengo, J. A., Soares, W. R., Saulo, C., and Nicolini, M.: Climatology of the low-level jet east of the Andes as derived from the NCEP-NCAR reanalyses: Characteristics and temporal variability, J. Climate, 17, 2261–2280, 2004.

Marengo, J. A.: Characteristics and spatio-temporal variability of the Amazon River Basin Water Budget, Clim. Dynam., 24, 11–22, 2005.

Marengo, J. A.: On the hydrological cycle of the Amazon basin: a historical review and current state-of-the-art, Revista Brasileira de Meteorologia, 21, 1–19, 2006.

Marengo, J. A., Nobre, C. A., Tomasella, J., Oyama, M. D., Sampaio de Oliveira, G., De Oliveira, R., Camargo, H., Alves, L. M., and Brown, I. F.: The drought of Amazonia in 2005, J. Climate, 21, 495–516, 2008.

Martinez, J. A., and Dominguez, F.: Sources of Atmospheric Moisture for the La Plata River Basin, J. Climate, doi:10.1175/JCLI-D-14-00022.1, in press, 2014.

Medvigy, D., Walko, R. L., and Avissar, R.: Effects of deforestation on spatiotemporal distributions of precipitation in South America, J. Climate, 24, 2147–2163, 2011.

Miguez-Macho, G. and Fan, Y.: The role of groundwater in the Amazon water cycle. 2. Influence on seasonal soil moisture and evapotranspiration, J. Geophys. Res., 117, D15114, doi:10.1029/2012JD017540, 2012.

Milo, R., Shen-Orr, S., Itzkovitz, S., Kashtan, N., Chklovskii, D., and Alon, U.: Network motifs: simple building blocks of complex networks, Science, 298, 824–827, 2002.

Monteith, J.: Evaporation and environment, Sym. Soc. Exp. Biol., 19, 205–234, 1965.

Morton, D. C., Nagol, J., Carabajal, C. C., Rosette, J., Palace, M., Cook, B. D., Vermote, E. F., Harding, D. J., and North, P. R. J.: Amazon forests maintain consistent canopy structure and greenness during the dry season, Nature, 506, 221–224, 2014.

Mu, Q., Zhao, M., and Running, S. W.: Improvements to a MODIS global terrestrial evapotranspiration algorithm, Remote Sens. Environ., 115, 1781–1800, 2011.

Mueller, B., Seneviratne, S.I., Jimenez, C.,Corti, T., Hirschi, M., Balsamo, G., Ciais, P., Dirmeyer, P., Fisher, J. B., Guo, Z., Jung, M., Maignan, F., McCabe, M. F., Reichle, R., Reichstein, M., Rodell, M., Sheffield, J., Teuling, A. J., Wang, K., Wood, E. F. and Zhang, Y.: Evaluation of global observations-based evapotranspiration datasets and IPCC AR4 simulations, Geophys. Res. Lett., 38, L06402, doi:10.1029/2010GL046230, 2011.

Mueller, B., Hirschi, M., Jimenez, C., Ciais, P., Dirmeyer, P. A., Dolman, A. J.,Fisher, J. B., Jung, M., Ludwig, F., Maignan, F., Miralles, D. G., McCabe, M. F., Reichstein, M., Sheffield, J., Wang, K., Wood, E. F., Zhang, Y. and Seneviratne, S. I.: Benchmark products for land evapotranspiration: LandFlux-EVAL multi-data set synthesis., Hydrol. Earth Syst. Sc., 17, 3707 – 3720, 2013.

Myers, N., Mittermeier, R. A., Mittermeier, C. G., Da Fonseca, G. A. B., and Kent, J.: Biodiversity hotspots for conservation priorities, Nature, 403, 853–858, 2000.

Nepstad, D. C., de Carvalho, C. R., Davidson, E. A., Jipp, P. H., Lefebvre, P. A., Negreiros, G. H., da Silva, E. D., Stone, T. A., Trumbore, S. E., and Vieira, S.: The role of deep roots in the hydrological and carbon cycles of Amazonian forests and pastures, Nature, 372, 666–669, 1994.

New, M., Hulme, M., and Jones, P.: Representing twentieth-century space-time climate variability. Part II: Development of 1901–96 monthly grids of terrestrial surface climate, J. Climate, 13, 2217–2238, 2000.

Newman, M. E. J.: Scientific collaboration networks. II. Shortest paths, weighted networks, and centrality, Phys. Rev. E, 64, 016132, doi:10.1103/PhysRevE.64.016132, 2001.

Nobre, C. A., Sellers, P. J., and Shukla, J.: Amazonian deforestation and regional climate change, J. Climate, 4, 957–988, 1991.

Nobre, P., Malagutti, M., Urbano, D. F., de Almeida, R. A., and Giarolla, E.: Amazon deforestation and climate change in a coupled model simulation, J. Climate, 22, 5686–5697, 2009.

Numaguti, A.: Origin and recycling processes of precipitating water over the Eurasian continent: experiments using an atmospheric general circulation model, J. Geophys. Res.-Atmos., 104, 1957–1972, 1999.

Oyama, M. D. and Nobre, C. A.: A new climate-vegetation equilibrium state for tropical South America, Geophys. Res. Lett., 30, 2199, doi:10.1029/2003GL018600, 2003.

Rockström, J., Falkenmark, M., Karlberg, L., Hoff, H., Rost, S., and Gerten, D.: Future water availability for global food production: the potential of green water for increasing resilience to global change, Water Resour. Res., 45, W00A12, doi:10.1029/2007WR006767, 2009.

Rozante, J. R. and Cavalcanti, I. F. A.: Regional Eta model experiments: SALLJEX and MCS development, J. Geophys. Res.-Atmos., 113, D17106, doi:10.1029/2007JD009566, 2008.

Rozante, J. R., Moreira, D. S., de Goncalves, L. G. G., and Vila, D. A.: Combining TRMM and surface observations of precipitation: technique and validation over South America, Weather Forecast., 25, 885–894, 2010.

Ruhoff, A.: Predicting evapotranspiration in tropical biomes using MODIS remote sensing data, Ph.D. thesis, Federal University of Rio Grande do Sul, Porto Alegre, 2011.

Salati, E., Dall'Olio, A., Matsui, E., and Gat, J. R.: Recycling of water in the Amazon basin: an isotopic study, Water Resour., 15, 1250–1258, doi:10.1029/WR015i005p01250, 1979.

Sampaio, G., Nobre, C., Costa, M. H., Satyamurty, P., Soares-Filho, B. S., and Cardoso, M.: Regional climate change over eastern Amazonia caused by pasture and soybean cropland expansion, Geophys. Res. Lett., 34, L17709, doi:10.1029/2007GL030612, 2007.

Savenije, H. H. G.: The importance of interception and why we should delete the term evapotranspiration from our vocabulary, Hydrol. Process., 18, 1507–1511, 2004.

Shukla, J., Nobre, C., and Sellers, P.: Amazon deforestation and climate change, Science, 247, 1322–1325, 1990.

Spracklen, D. V., Arnold, S. R., and Taylor, C. M.: Observations of increased tropical rainfall preceded by air passage over forests, Nature, 489, 282–285, 2012.

Sudradjat, A., Brubaker, K., and Dirmeyer, P.: Precipitation source/sink connections between the Amazon and La Plata River basins, in: AGU Fall Meeting Abstracts, vol. 1, p. 0830, San Francisco, California, 6–10 December 2002.

Trenberth, K. E.: Atmospheric moisture recycling: role of advection and local evaporation, J. Climate, 12, 1368–1381, 1999.

Tsonis, A. A., Swanson, K. L., and Wang, G.: On the role of atmospheric teleconnections in climate, J. Climate, 21, 2990–3001, 2008.

van der Ent, R. J., Savenije, H. H. G., Schaefli, B., and Steele-Dunne, S. C.: Origin and fate of atmospheric moisture over continents, Water Resour. Res., 46, W09525, doi:10.1029/2010WR009127, 2010.

van der Ent, R. J. and Savenije, H. H. G.: Length and time scales of atmospheric moisture recycling, Atmos. Chem. Phys., 11, 1853–1863, doi:10.5194/acp-11-1853-2011, 2011.

van der Ent, R. J., Tuinenburg, O. A., Knoche, H.-R., Kunstmann, H., and Savenije, H. H. G.: Should we use a simple or complex model for moisture recycling and atmospheric moisture tracking?, Hydrol. Earth Syst. Sci. Discuss., 10, 6723–6764, doi:10.5194/hessd-10-6723-2013, 2013.

van der Ent, R. J., Wang-Erlandsson L., Keys P. W., and Savenije H. H. G.: Contrasting roles of interception and transpiration in the hydrological cycle – Part 2: Moisture recycling, Earth Syst. Dynam. Discuss., 5, 281–326, 2014.

Vera, C., Baez, J., Douglas, M., Emmanuel, C. B., Marengo, J., Meitin, J., Nicolini, M., Nogues-Paegle, J., Paegle, J., Penalba, O., Salio, P., Saulo, C., Silva Dias, M. A., Silva Dias, P., and Zipser, E.: The South American low-level jet experiment, B. Am. Meteorol. Soc., 87, 63–77, 2006.

Victoria, R. L., Martinelli, L. A., Mortatti, J., and Richey, J.: Mechanisms of water recycling in the Amazon basin: isotopic insights, Ambio, 20, 384–387, 1991.

Walker, R., Moore, N. J., Arima, E., Perz, S., Simmons, C., Caldas, M., Vergara, D., and Bohrer, C.: Protecting the Amazon with protected areas, P. Natl. Acad. Sci. USA, 106, 10582–10586, 2009.

Werth, D. and Avissar, R.: The local and global effects of Amazon deforestation, J. Geophys. Res.-Atmos., 107, 1322–1325, 2002.

Zemp, D. C., Wiedermann, M., Kurths, J., Rammig, A., and Donges, J. F.: Node-weighted measures for complex networks with directed and weighted edges for studying continental moisture recycling, Europhys. Lett., 107, 58005, doi:10.1209/0295-5075/107/58005, 2014.